Vangl2 suppresses NF-κB signaling and ameliorates sepsis by targeting p65 for NDP52-mediated autophagic degradation

Jiansen Lu[1,2,10], Jiahuan Zhang[3,10], Huaji Jiang[2,4,10], Zhiqiang Hu[2,10], Yufen Zhang[2], Lian He[5,6], Jianwu Yang[2], Yingchao Xie[2], Dan Wu[2], Hongyu Li[2], Ke Zeng[2], Peng Tan[5,7], Qingyue Xiao[8], Zijing Song[8], Chenglong Pan[1], Xiaochun Bai[8*] and Xiao Yu[2,3,9*]

[1]Department of Joint Surgery, the Fifth Affiliated Hospital, Southern Medical University, Guangzhou, Guangdong 510515, China

[2]Department of Immunology, School of Basic Medical Sciences, Southern Medical University, Guangzhou, Guangdong 510515, China

[3]Department of Clinical Laboratory Medicine, Guangdong Provincial People's Hospital (Guangdong Academy of Medical Sciences), Southern Medical University, Guangzhou, Guangdong 510515, China

[4]Department of Orthopaedics, Yuebei People's Hospital Affiliated to Medical College of Shantou University, Shaoguan 512026, China

[5]Department of Pharmacology, School of Medicine, Southern University of Science and Technology, Shenzhen, Guangdong 518005, China

[6]Institute of Biosciences and Technology, College of Medicine, Texas A&M University, Houston, Texas 77030, USA

[7]Klarman Cell Observatory, Broad Institute of MIT and Harvard, Cambridge, Massachusetts 02142, USA

[8]Department of Cell Biology, School of Basic Medical Sciences, Southern Medical University, Guangzhou, Guangdong 510515, China

[9]Guangdong Provincial Key Lab of Single Cell Technology and Application, Southern Medical University, Guangzhou, Guangdong 510515, China

[10]These authors contribute equally.

*Correspondence: X.Y. (xiaoyu523@smu.edu.cn), X.B. (baixc15@smu.edu.cn)

Abstract

Van Gogh-like 2 (Vangl2), a core planar cell polarity (PCP) component, plays an important role in polarized cellular and tissue morphology induction, growth development and cancer. However, its role in regulating inflammatory responses remains elusive. Here, we report that Vangl2 is upregulated in patients with sepsis and identify Vangl2 as a negative regulator of NF-κB signaling by regulating the protein stability and activation of the core transcription component p65. Mice with myeloid-specific deletion of Vangl2 (*Vangl2*$^{\Delta M}$) are hypersusceptible to lipopolysaccharide (LPS)-induced septic shock. Vangl2 deficient myeloid cells exhibit enhanced phosphorylation and expression of p65, therefore, promoting the secretion of pro-inflammatory cytokines after LPS stimulation. Mechanistically, NF-κB signaling-induced-Vangl2 recruits E3 ubiquitin ligase PDLIM2 to catalyze K63-linked ubiquitination on p65, which serves as a recognition signal for cargo receptor NDP52-mediated selective autophagic degradation. Taken together, these findings demonstrate Vangl2 as a suppressor of NF-κB mediated inflammation and provide insights into the crosstalk between autophagy and inflammatory diseases.

Introduction

Vangl2, a core PCP component, mediates Wingless-type (Wnt)/PCP signaling, and controls homeostasis, development, and repair of organs (Bailly, Walton, & Borg, 2018; Brunt et al., 2021; Hatakeyama, Wald, Printsev, Ho, & Carraway, 2014). Vangl2 has four transmembrane domains with both carboxyl termini and amino oriented toward the cytoplasm, which is phosphorylated in the endoplasmic reticulum (ER) and then transported to the cell surface and becomes stabilized, while the unphosphorylated Vangl2 is unstable and internalized to degrade via the lysosomal pathway (D. Feng et al., 2021). The shuttle of Vangl2 between cytoplasm and cell membrane results in its multifunction, including adhesion, membrane protrusive activity, migration, and bridging proteins (Hatakeyama et al., 2014). Indeed, Vangl2 inhibited matrix metalloproteinase 2 (MMP2) activity and affected cell adhesion to extracellular matrix proteins (Jessen & Jessen, 2017). Vangl2 also modulates glomerular injury by promoting MMP9 (Papakrivopoulou et al., 2018). Moreover, the abnormal function of Vangl2 results in various diseases, such as cancer, kidney glomerular injury, idiopathic pulmonary fibrosis and systemic dysplasia (Papakrivopoulou et al., 2018; Poobalasingam et al., 2017). Vangl2 is markedly down-regulated in patients with emphysema (Poobalasingam et al., 2017), while which level was up-regulated and amplified in breast, ovarian, and uterine carcinomas (Cancer Genome Atlas Research et al., 2013; Cerami et al., 2012; Gao et al., 2013). In addition, Vangl2 is bounded to p62 to promote breast cancer (Puvirajesinghe et al., 2016). Our previous study showed that Vangl2 prevents osteogenic differentiation in mesenchymal stem cells, resulting in osteogenic dysplasia (Gong et al., 2021). Vangl2 mediated downstream factors of Toll-like or interleukin (IL)-1 receptor, such as myeloid differentiation factor 88 (MyD88) (Gong et al., 2021), suggesting that Vangl2 may play roles in immune-related diseases, including autoimmune diseases. However, the function of Vangl2 in inflammatory diseases remains uncovered.

The NF-κB signaling is critical for the pathogenesis of a number of inflammatory diseases, such as inflammatory bowel disease (IBD), rheumatoid arthritis (RA), systemic lupus erythematosus (SLE) and sepsis (Liu, Zhang, Joo, & Sun, 2017). NF-κB activation relies on the pattern recognition receptors (PRRs) recognition of pathogen-associated molecular patterns (PAMPs), including Toll like receptor (TLR), NOD-like receptors (NLRs) and RIG-I-like receptors (RLRs) (Liu et al., 2017). LPS triggers TLR activation and the recruitment of adaptor proteins including MyD88. This in turn activates a series

of downstream canonical NF-κB signaling cascade, resulting in the phosphorylation and degradation of IκB and the nuclear translocation of RelA/p65 and p50 to induce the transcription of several inflammatory cytokines, such as interleukin (IL)-1, IL-6, and tumor necrosis factor-α (TNF-α) (Funes, Rios, Escobar-Vera, & Kalergis, 2018; Locati, Curtale, & Mantovani, 2020). Since uncontrolled immune responses are detrimental to the host, inappropriate or excessive NF-κB activity contributes to the pathogenesis of various inflammatory diseases and cancer (Cartwright, Perkins, & C, 2016). Thus NF-κB signaling must be tightly regulated to maintain immune balance in the organism. In recent decades, extensive studies have focused on the mechanisms underlying the regulation of NF-κB signaling. Recent research demonstrated that NLRC5 strongly prevents NF-κB signaling pathway by interacting with IκB kinase (IKK) α/IKKβ and blocking their phosphorylation (Cui et al., 2010). COMMD1, PPARγ, SOCS1 and GCN5 were also shown to negatively regulate NF-κB signaling (Bartuzi, Hofker, & van de Sluis, 2013; Mao et al., 2009). Meanwhile, tripartite motif-containing protein 21 (Trim21) enhanced the interaction of p65 with IKK, which promotes p65 phosphorylation and downstream gene activation (Yang et al., 2021). However, the molecular mechanisms underpinning the regulation of NF-κB signaling are still elusive.

Autophagy, a conserved intracellular degradation pathway, decomposes cytoplasmic organelles and components, and acts as a defense mechanism to pathogen infection, playing a crucial role in nutrient recycling, stress response and cellular homeostasis (Ashrafi & Schwarz, 2013; Denton & Kumar, 2019). Recent evidence indicates that autophagy is highly selective when delivering specific substrates to autolysosomal degradation by virtue of a number of cargo receptors, including sequestosome 1 (SQSTM1/p62), optineurin (OPTN), nuclear dot protein 52 (NDP52/CALCOCO2) and neighbor of BRCA1 (NBR1) (Gatica, Lahiri, & Klionsky, 2018). Selective autophagy targets immune regulators for degradation, thus suppressing innate immune signaling, such as type I IFN and NF-κB signaling (Pradel, Robert-Hebmann, & Espert, 2020; Tong et al., 2012). Moreover, p62 protein has been identified as a novel Vangl2-binding partner (Puvirajesinghe et al., 2016), and our recent study has demonstrated that Vangl2 reduces lysosomal chaperone-mediated autophagy (CMA) activity by targeting LAMP-2A for degradation (Gong et al., 2021). However, whether and how Vangle2 is involved in the selective autophagic regulation of NF-κB signaling remains largely unknown.

In this study, we uncover a previously unrecognized role of Vangl2, as a “molecular brake”, in the negative regulation of NF-κB signaling to prevent excessive and potentially harmful immune responses during sepsis in both human patient samples and LPS induced mouse model. Induction of Vangl2 upon inflammation recruits an E3 ubiquitin ligase PDLIM2 to catalyze K63-linked ubiquitination on p65, thus promoting the recognition of p65 by the cargo receptor NDP52 and resulting in the selective autophagic degradation of p65. Our findings provide a potential target for the treatment of inflammatory diseases.

Results

Loss of Vangl2 promotes inflammatory responses in LPS-induced septic shock.

To investigate the potential role of Vangl2 in inflammatory response, we first analyzed the expression of Vangl2 in peripheral blood mononuclear cells (PBMCs) from sepsis patients (Fig. S1 A) and found mRNA level of Vangl2 was increased in the sepsis patients compared to healthy control (HC) (Fig. 1 A). Moreover, the serum of the high Vangl2 expression group had lower levels of IL-6, white blood cell (WBC), and acute C-reactive protein (CRP) than the low Vangl2 expression group (Fig. S1 A). Expression of Vangl2 from database GSE156382 also confirmed that Vangl2 mRNA was induced during sepsis (Fig. S1 B). To further determine whether *Vangl2* expression could be regulated in response to inflammatory stimulation, we treated mice with LPS to activate NF-κB pathway and detected *Vangl2* mRNA in different tissues from LPS treated mice, and found the expression of *Vangl2* significantly increased in secondary lymphoid organs including the spleen and lymph nodes after LPS stimulation, but not in other tissues (Fig. 1 B). Moreover, qPCR and western blot analyses revealed strong upregulation of *Vangl2* at both the mRNA and protein levels after LPS stimulation in bone marrow (BM)-derived macrophages (BMDMs), neutrophils and peritoneal macrophages (pMACs) (Fig. S1, C-E), suggesting that Vangl2 is induced in immune organ tissues and cells in response to inflammation.

To determine the function of Vangl2 during LPS-induced sepsis, we specifically ablated Vangl2 in myeloid cells by crossing *Vangl2*$^{flox/flox}$ mice with mice expressing lysozyme proximal promoter (*Lyz2-Cre*). The resultant homozygous *Vangl2*$^{flox/flox}$ × *Lyz2-Cre* mice were designated *Vangl2*$^{\Delta M}$ mice and selective deletion of Vangl2 in myeloid cells of *Vangl2*$^{\Delta M}$ mice were confirmed by PCR (Fig. S1 F). Although there were no significant differences in the size of spleen and lymph nodes between wild-type (WT)

and *Vangl2*$^{\Delta M}$ mice (Fig. S1 G), myeloid-specific loss of Vangl2 increased the number of monocytes, macrophages and neutrophils in the spleen and bone marrow (Fig. S1, H and I). To gain further insight into the physiological function of Vangl2, we treated WT and *Vangl2*$^{\Delta M}$ mice with a high dose of LPS and monitored mice survival. We found that all *Vangl2*$^{\Delta M}$ mice died after LPS-induced septic shock within 20 hours, compared to only 20% of the WT mice, whereas the remaining WT mice survived for more than 50 hours (Fig. 1 C). Consistent with this observation, *Vangl2*$^{\Delta M}$ mice markedly increased the protein level of IL-1β in isolated CD11b^{+} splenocytes (Fig. 1 D), and mRNA levels of *Il1b*, *Tnfa* and *Il6* in the spleen (Fig. 1 E). Meanwhile, *Vangl2*$^{\Delta M}$ mice showed markedly elevated serum amounts of proinflammatory cytokines such as IL-1β, TNF-α and IL-6 after LPS treatment, compared with WT mice (Fig. 1 F). Together, these data provide in vivo evidence that myeloid cell-specific deletion of Vangl2 in mice enhances the sensitivity and severity of LPS-induced septic shock and is associated with increased expression of proinflammatory cytokines.

Vangl2 negatively regulates NF-κB activation and inflammation in myeloid cells.

To investigate the mechanisms by which Vangl2 prevents sepsis, we performed RNA-seq analysis to identify signal pathways involved in LPS-induced septic shock by comparing LPS-stimulated BMDMs from *Vangl2*$^{\Delta M}$ and WT mice. Results showed 907 up-regulated genes (including inflammatory cytokines) and 1092 down-regulated genes in response to Vangl2 deficiency in BMDMs after LPS stimulation (Fig. S2 A). Consistent with Fig. 1, gene ontology (GO) analysis further identified that these genes are involved in cellular immune responses, including “cellular response to lipopolysaccharide” (Fig. S2 B). Moreover, KEGG analysis revealed genes involved in TNF signaling pathway and cytokine-cytokine receptor interaction were highly enriched in *Vangl2*$^{\Delta M}$ BMDMs after LPS stimulation, suggesting that Vangl2 may regulate these signaling pathways and related cytokines release (Fig. S2 C).

To determine the function of Vangl2 in innate immune signaling in myeloid cells, we isolated BMDMs, neutrophils and pMACs from WT and *Vangl2*$^{\Delta M}$ mice, treated them with LPS, and performed immunoblot analysis with specific antibodies. We found that phosphorylations of p65 were enhanced and remained high level for a sustained period in Vangl2-deficient pMACs and neutrophils, compared with WT cells (Fig. 2, A-D). Consistent with this observation, Vangl2-deficient macrophages, and neutrophils showed markedly elevated pro-inflammatory cytokines such as TNF-α, IL-6 (Fig. 2 E and F and

Fig. S2 D and E) and IL-1β (Fig. S2 F), after LPS treatment. Moreover, we detected enhanced p65 nuclear accumulation in LPS-induced Vangl2-deficient neutrophils, compared with WT neutrophils (Fig. 2, G and H).

To further confirm the function of Vangl2 in regulating NF-κB signaling, we overexpressed Flag-tagged Vangl2 in A549 cells. We found that Vangl2 overexpression inhibited phosphorylation of p65 in A549 cells (Fig. 2, I and J). These results suggest that Vangl2 prevents LPS-induced NF-κB activation and proinflammatory cytokine production.

Vangl2 inhibits LPS-induced NF-κB activation by interacting with p65.

To clarify the regulatory mechanism of Vangl2, we transfected Chinese hamster ovary (CHO) or 293T cells with NF-κB luciferase reporter vector, with or without the Vangl2 plasmid, then treated the cells with LPS, IL-1β, or TNF-α. We found that Vangl2 markedly inhibited NF-κB activation induced by LPS, IL-1β, or TNF-α in a dose-dependent manner (Fig. 3, A-C). Next, we sought to determine potential signaling molecules that mediated the NF-κB-luc reporter. NF-κB-luc activity was strongly activated by overexpression of MyD88, IRAK1, TRAF6, IKKα, IKKβ or p65, but all of these activities were inhibited when *Vangl2* was co-transfected at increasing concentrations (Fig. 3 D and Fig. S3, A-F), suggesting that Vangl2 may block NF-κB activation at the very downstream signaling level of p65.

To test this prediction, we transfected 293T cells with HA-tagged Vangl2 together with Flag-tagged IKKα, IKKβ, p65, TRAF6, IRAK1 or MyD88. Co-immunoprecipitation (co-IP) assay revealed that Vangl2 interacted strongly with IKKα, IKKβ, p65 and MyD88 (Fig. 3 E and Fig. S3 G, H). In addition, endogenous co-IP immunoblot analyses showed that Vangl2 was strongly associated with p65 upon LPS stimulation in BMDMs, but not with IKKα, IKKβ or MyD88 (Fig. 3 F and Fig. S3 I). Moreover, ZDOCK server predicted that Vangl2 may potentially interact with p65 by a hydrogen bond (Fig. S3 J). We further investigated the co-localization of Vangl2 and p65 by confocal microscopy and found a weak-co-localization of Vangl2 with p65 in unstimulated cells and the co-localization between Vangl2 and p65 was notably enhanced upon LPS stimulation (Fig. 3 G and Fig. S3 K). To determine how Vangl2 interacts with cytoplasmic p65, we isolated cytoplasm and membrane in LPS treated THP-1 cells. We found that Vangl2 interacted with p65 mainly in the cytoplasm, although most of Vangl2 located on the membrane (Fig. S3 L).

Together, these data suggest that Vangl2 may interact with p65 in the cytoplasm to inhibit NF-κB signaling.

Vangl2 comprises an N-terminal cytoplasmic tail (NT), a transmembrane (TM) domain, a Prickle-binding domain (PkBD), and a C-terminal cytoplasmic tail (CT) (Nagaoka, Furuse, Ohtsuka, Tsuchida, & Kishi, 2019). To map the essential domains of Vangl2 that mediate its association with p65, we generated several deletion constructs of Vangl2. We found Vangl2 FL (full-length), T2 (ΔNT+TM), T3 (ΔCT), and T4 (ΔNT) interacted with the full-length p65, while Vangl2 T1 (ΔPkBD+CT) abrogated their association (Fig. 3 H and Fig. S3 M), indicating that the PkBD domain is important for the Vangl2-p65 interaction. Additionally, we constructed HA-tagged Vangl2 PkBD plasmid and co-IP assay revealed that Vangl2 FL and PkBD interacted with p65 (Fig. 3 I). Moreover, we observed that deletion of the PkBD domain (T1), but not other domains, of Vangl2 abolished the Vangl2-mediated inhibition of NF-κB-luc activity, and transfection of Vangl2 PkBD domain achieved similar inhibition on p65 induced NF-κB activation as Vangl2 FL did (Fig. 3 J). Collectively, these data suggest that Vangl2 suppresses NF-κB signaling by targeting p65 through Vangl2 PkBD domain interaction.

Vangl2 promotes the autophagic degradation of p65.

Next we sought to study the physiological role of Vangl2-p65 interaction in the regulation of NF-κB signaling by transfecting 293T cells with Flag-tagged p65, together with increasing doses of Vangl2, and found that Vangl2 dramatically decreased the protein level of p65 in a dose-dependent manner (Fig. 4 A). To exclude the possibility that the downregulation of p65 protein by Vangl2 was caused by the inhibition of p65 transcription, qPCR results suggested that the abundance of *p65* mRNA did not change in cells with increased expression of Vangl2 (Fig. 4 B). Moreover, Vangl2 facilitated the degradation of the p65 phosphorylation mutants (Fig S4A), and Vangl2 phosphorylation mutants were observed to degrade p65 (Fig S4B), indicating that Vangl2 mediated p65 degradation is independent of its phosphorylation status. Since activated p65 translocates to the nucleus, we next assessed whether Vangl2 regulates the degradation of p65 in the cytoplasm or nucleus, and found that the Vangl2 interacted with p65 mainly in the cytoplasm (Fig. S4 C) and mediated the degradation of p65 in the cytoplasmic fraction (Fig. 4 C), which is consistent with the result that Vangl2 and p65 co-localized in the cytoplasm (Fig. 3 G). To further assess whether Vangl2 regulates the degradation of endogenous p65, we found that Vangl2-deficient BMDMs stabilized the expression of

endogenous p65 after LPS treatment (Fig. 4 D). After 12 h of LPS stimulation, the cycloheximide (CHX)-chase assay result showed that the degradation rate of p65 in *Vangl2*$^{\Delta M}$ BMDMs was slower than that of WT cells (Fig. S4 D). Together, these data suggest that Vangl2 promotes p65 protein degradation.

To investigate whether Vangl2 degrades p65 through an autolysosome or proteasome pathway, 293T cells were transfected with p65, together with or without the Vangl2 plasmids, and treated with different pharmacological inhibitors. We found the degradation of p65 induced by Vangl2 was blocked by autolysosome inhibitor chloroquine (CQ) and bafilomycin A1 (Baf A1), or autophagy inhibitor 3-methyladenine (3-MA) (Fig. 4 E), but not by the proteasome inhibitor MG132 or caspase-1 inhibitor Z-VAD and VX-765 (Fig. 4 E and Fig. S4 E). Furthermore, Vangl2 significantly increased the degradation of p65 during rapamycin-triggered autophagy (Fig. 4 F), which suggested that Vangl2 promoted autophagic degradation of p65.

To further demonstrate Vangl2 mediated p65 degradation through autophagy, we transfected WT, ATG5, and Beclin1 knockout (KO) 293T cells with Vangl2, and found that the degradation of p65 triggered by Vangl2 was almost abrogated in ATG5 and Beclin1 KO cells (Fig. 4 G). The p65 turnover rates were markedly reduced in ATG5 and Beclin1 KO cells post CHX treatment (Fig. S4, F and G), suggesting that the impaired autophagy prevented p65 degradation. Consistently, NF-κB activation induced by p65 was rescued in ATG5 and Beclin1 KO cells expressing Vangl2, compared to WT 293T cells (Fig. 4, H and I). In addition, the colocalization of p65 and LC3B was enhanced following LPS stimulation (Fig. S4, H). Together, our data suggest that Vangl2 specifically promotes p65 degradation through autophagy.

Vangl2 promotes the recognition of p65 by cargo receptor NDP52.

Accumulating evidence showed that cargo receptors play crucial roles in selective autophagic degradation by delivering substrates (X. He et al., 2019; Kirkin & Rogov, 2019; Wu et al., 2021). Since there is no research suggests that Vangl2 is a cargo protein, we hypothesized that Vangl2 might bridge p65 to the cargo receptors for autophagic degradation. To identify the potential cargo receptor responsible for Vangl2-mediated autophagic degradation of p65, we co-transfected 293T cells with Vangl2 and various cargo receptors, followed by Co-IP assay. Result suggested that Vangl2 strongly interacted with the cargo receptors p62 and NDP52, and slightly associated with NBR1 and Nix (Fig. 5 A). However, p65 only interacted with the cargo receptors p62 and

NDP52 (Fig. 5 B), which is consistent with a recent finding that p62 protein is a Vangl2-binding partner (Puvirajesinghe et al., 2016). We next attempted to clarify whether p62 or NDP52 is involved in Vangl2-mediated autophagic degradation of p65. Interestingly, we found that Vangl2 promoted the association between p65 and NDP52, but did not affect p65-p62 complex (Fig. 5 C). Consistently, we found that Vangl2 mediated degradation of p65 was rescued in NDP52 KO cells, but not in p62 KO cells (Fig. 5 D). Endogenous co-IP immunoblot analyses also revealed that deficiency of Vangl2 remarkably attenuated the association of endogenous p65 and NDP52 (Fig. 5 E). Likewise, NDP52, but not p62, enhanced the association between p65 and Vangl2 (Fig. 5 F and Fig. S5 A). And Vangl2 failed to inhibit the activation of NF-κB signaling in NDP52 KO cells (Fig. 5 G), but not in p62 KO cells (Fig. S5 B). Furthermore, compared with WT cells, CHX-chase assay results showed that the degradation rates of p65 were reduced in NDP52 KO cells (Fig. 5 H), but not in p62 KO cells (Fig. S5 C). Taken together, these data suggest that Vangl2 mediates the NDP52-directed selective autophagic degradation of p65.

Vangl2 increases the K63-linked poly-ubiquitination of p65.

It has been well documented that ubiquitin chains attached to the substrates and served as a signal for the recognition by cargo receptors (Otten et al., 2021; Shaid, Brandts, Serve, & Dikic, 2013; Yin, Popelka, Lei, Yang, & Klionsky, 2020). The ubiquitin-associated (UBA) domain of NDP52 mostly recognized ubiquitinated substrates for degradation through autophagy (Johansen & Lamark, 2014; Yamano & Youle, 2020). We hypothesized that Vangl2 may affect the ubiquitin chains on p65 for subsequent NDP52-dependent degradation. To demonstrate this, we performed endogenous co-IP assay and found that the poly-ubiquitination of p65 was impaired in BMDMs from *Vangl2*$^{\Delta M}$ mice after LPS stimulation, compared to WT mice (Fig. 6 A). Moreover, Vangl2 specifically increased the total and K63-linked (K63-only ubiquitin mutant) poly-ubiquitination of p65 (Fig. 6 B). In contrast, Vangl2 did not affect other ubiquitin linkages (K11, K27, K33, or K48-only ubiquitin mutant) of p65 in an overexpression system (Fig. 6 C). To further substantiate the hypothesis that Vangl2 is involved in K63-linked poly-ubiquitinated p65, we conducted a knockdown experiment using siRNA to reduce Vangl2 expression. Our results demonstrated that the absence of Vangl2 inhibits K63-linked poly-ubiquitination of p65 (Fig. 6 D). Together, these results suggest that Vangl2 promotes the degradation of p65 by promoting the K63-linked ubiquitination of p65.

Vangl2 recruits PDLIM2 to ubiquitinate p65.

Although Vangl2 promotes K63-linked ubiquitination and degradation of p65, Vangl2 is not an E3 ubiquitin ligase. We hypothesized that Vangl2 might function as a scaffold protein to link p65 and its E3 ubiquitin ligase for ubiquitination or to block the interaction of deubiquitinase (DUB) with p65. To identify the potential E3 ubiquitinase or DUB responsible for Vangl2 mediated ubiquitination of p65, we further analyzed our RNA-seq data to identify E3 ubiquitin ligase or DUB involved in ubiquitination of p65 by comparing LPS-stimulated BMDMs from *Vangl2*$^{\Delta M}$ and WT mice. The result of differentially expression identified 88 down-regulated genes related to E3 ubiquitin ligase and 56 up-regulated genes related to DUB in response to Vangl2 deficiency in BMDMs after LPS stimulation (Fig. S6 A), which included PDZ-LIM domain-containing protein 2 (PDLIM2), Trim21 and DUB ubiquitin-specific peptidase 7 (USP7). Recent research showed that ubiquitin E3 ligases PDLIM2 and Trim21 ubiquitinated p65 via K63 linkage and enhanced the interaction of p65 with IKK (Healy & O'Connor, 2009; Jodo, Shibazaki, Onuma, Kaisho, & Tanaka, 2020; Yang et al., 2021), while DUB USP7 promoted NF-κB-mediated transcription (Mitxitorena et al., 2020). Here, we found that the mRNA level of PDLIM2 and USP7 decreased in Vangl2-deficient BMDMs, compared with WT BMDMs (Fig. S6, B-D). To investigate which E3 ubiquitin ligase or DUB is recruited by Vangl2, luciferase assay in Vangl2-expressing 293T cells transfected with scramble, *Pdlim2*, *Usp7*, or *Trim21* siRNA (Fig. S6, E-G) suggested Vangl2-mediated inhibition of NF-κB activation and degradation of p65 were blocked by knocking down PDLIM2, but not USP7 or Trim21 (Fig. 7 A). Meanwhile, *Pdlim2* knockdown in BMDMs also resulted in higher expression of *Il6* and *Il1b* in response to LPS stimulation (Fig. 7, B and C), indicating that PDLIM2 plays a key role in promoting Vangl2-mediated p65 degradation.

We next investigated whether Vangl2 promoted the association between p65 and PDLIM2 by co-IP experiments. Our results indicated that Vangl2 interacted with PDLIM2 (Fig. 7 D) and promoted the association between p65 and PDLIM2 (Fig. 7 E). Notably, PDLIM2 accelerated the degradation of p65 in the presence of Vangl2 (Fig. 7 F). Conversely, PDLIM2 deficiency markedly impaired Vangl2-mediated K63-linked ubiquitination of p65 (Fig. 7 G) and knockdown of Vangl2 inhibited K63-linked poly-ubiquitination of p65 mediated by PDLIM2 (Fig. 7 H). Taken together, these data suggest that Vangl2 functions as a potential adaptor to recruit E3 ubiquitin ligase

PDLIM2 to p65 and promotes the K63-linked ubiquitination of p65 for its subsequent autophagic degradation.

Discussion

As a core PCP component, Vangl2 is widely known for its function in organ development, such as brain, tooth, tongue and kidney (Bailly et al., 2018; Hatakeyama et al., 2014), trafficking from the endoplasmic reticulum (ER) to the cell surface, and subsequently shuttles between the endocytic vesicles and cell surface (D. Feng et al., 2021). The function of Vangl2 mostly depends on its cellular localization (Hatakeyama et al., 2014) and is reported mainly through PCP/WNT signaling pathway (Jessen & Jessen, 2019). Activated Vangl2 exhibits extremely long cytoplasmic and intercellular branches and delivers Wnt to multiple cells to enhance Wnt/β-Catenin signaling (Brunt et al., 2021). During myocardial hypertrophy, Vangl2 aggravates myocardial hypertrophy by regulating Wnt/JNK signaling (Brunt et al., 2021; Jessen & Jessen, 2017, 2019) and the expansion of cardiomyocyte surface area (Brunt et al., 2021; Jessen & Jessen, 2017, 2019). However, our previous study showed that the lysosome-suppressing function of Vangl2 in osteoblast differentiation is not dependent on conventional PCP pathway (Gong et al., 2021) , and we found Vangl2 did not affect the JNK pathway after LPS treatment (data no shown), suggesting that Vangl2 has additional functions in pathways besides PCP. In this study, we provided direct evidence that the expression of Vangl2 was increased during sepsis and upregulated significantly in immune organs (lymph nodes and spleen) upon LPS stimulation, which is consistent with our previous finding that Vangl2 regulated the downstream signaling of TLR or IL-1R. In addition, the present study showed that Vangl2 prevented the progression of sepsis and the accumulation of inflammatory cytokines through suppressing NF-κB pathway: Vangl2 inhibited LPS-induced NF-κB activation by delivering p65 to autophagosome for degradation. To the best of our knowledge, this is the first study proves that Vangl2 regulates NF-κB signaling and inflammatory responses, and could serve as a potential target for therapeutic purposes in diseases associated with NF-κB signaling.

As is well-known, Vangl2 phosphorylation is essential for its functions in the mammalian PCP pathway in multiple tissues. However, our findings indicate that Vangl2 phosphorylation mutants also promote p65 degradation (Fig. S4 B) and the degradation of p65 induced by Vangl2 was blocked by autolysosome inhibitor (CQ), but not by the JNK inhibitor (SP600125) or Wnt/β-catenin inhibitor (FH535) (data no shown),

suggesting that Vangl2 may regulate the NF-κB pathway independently of its conventional PCP pathway. Nevertheless, additional pathway inhibitions, such as those of the HH/GLI and Fat-Dachsous pathways, should also be employed to further elucidate the function of Vangl2 in p65 degradation. The PCP pathways frequently intersect with developmentally important pathways. Previous research has demonstrated that Vangl2 deficiency can affect developmental processes. It would be importance to investigate whether Vangl2-dependent NF-κB is influenced by developmental pathways. Distinct from previous studies, our findings revealed no significant differences in spleen and lymph node size between wild-type (WT) and *Vangl2*$^{\Delta M}$ mice. However, myeloid-specific loss of Vangl2 resulted in increased numbers of monocytes, macrophages, and neutrophils in the spleen and bone marrow. This suggests that the ablation of Vangl2 in myeloid cells does not affect the development of immune system development, but rather affects the differentiation of specific cell types. Moreover, we found that Vangl2 is induced and functions under LPS stimulation. Collectively, these findings suggest that Vangl2-dependent NF-κB functions do not affect the development of the immune system, but rather influence the progression of inflammatory-related diseases.

In our study, LPS stimulation did not mediate the expression of Vangl2 in the lungs and liver, though there are lots of resident immune cells in these organs, which suggests that Vangl2 may be important in circulating immune cells and not in the resident population. Given that LPS stimulation markedly alters the expression of Vangl2 in lymph nodes and spleen, rather than in the lungs and liver, we concentrated on the function of Vangl2 in myeloid cells. However, the restricted tissue-specificity of the interaction between two ubiquitously present proteins remains a challenge to comprehend and further investigation is needed.

The proteasome, lysosome and autolysosome pathways are the major systems that are utilized by eukaryotic cells to maintain the protein abundance and immune homeostasis (Deretic, 2021). Previous studies have shown that cellular levels of Vangl2 (D. Feng et al., 2021) and its binding partner Prickle2 (Nagaoka et al., 2019) are maintained by the proteasomal pathway. Our recent study showed that Vangl2 mediated osteogenic differentiation by limiting chaperone-mediated autophagy (CMA) in mesenchymal stem cells, suggesting a potential close relationship between Vangl2 and autophagy (Gong et al., 2021). Moreover, Vangl2 interacts with LAMP-2A through PkBD domain. Interestingly, we also found Vangl2 interacted with p65 through PkBD domain, indicating that the PkBD domain of Vangl2 play a pivotal role in mediating the interaction

between Vangl2 and its target protein. Furthermore, our study suggests Vangl2 promotes p65 degradation through autophagy pathway, but not proteasomal pathway. Importantly, we demonstrated that the degradation of p65 mediated by Vangl2-NDP52 complex is regulated by autophagy induction through rapamycin treatment and autophagy blockade by ATG5 KO or Beclin1 KO. Considering our findings and previous reports, Vangl2 may play multi-functional roles in regulating different types of autophagy (i.e. CMA or selective autophagy).

Selective autophagy requires that cargo receptors recognize the labeling of cargoes with degradation signals and subsequently engaged with the LC3 localized in the autophagosome membrane (Shaid et al., 2013). Common cargo receptors mainly include p62/SQSTM1, CALCOCO2/NDP52, OPTN, NBR1 and TOLLIP (Johansen & Lamark, 2014; Yamano & Youle, 2020). A study in HEK293T cells showed that LRRC25 promotes the autophagic degradation of p65 through enhancing the interaction between p65 and p62 (Y. Feng et al., 2017). In addition, a recent study showed that Vangl2 interacts with p62, subsequently promoting breast tumors by activating JNK signaling (Puvirajesinghe et al., 2016). Thus, we hypothesized that Vangl2 may promote the autophagic degradation of p65 by recruiting the cargo receptor p62. However, our data suggested that Vangl2 markedly increased the p65-NDP52 interaction but not p65-p62. Strikingly, Vangl2 mediated autophagic degradation of p65 was abolished in NDP52 KO cells, but not in p62 KO cells. Thus, our findings identify that NDP52 is the new cargo receptor responsible for Vangl2-mediated selective autophagic degradation of p65.

Accumulating evidence has shown that cargo receptors mainly recognize ubiquitination modifications on the substrates and then promote degradation in auto-lysosome (Shaid et al., 2013). As expected, we observed Vangl2 promoted the ubiquitination of p65, thus enhancing the association between cargo protein and p65. K48- and K63-linked ubiquitination were mostly reported modifications on p65 (Kauppinen, Suuronen, Ojala, Kaarniranta, & Salminen, 2013; Korbecki, Bobinski, & Dutka, 2019). For example, E3 ubiquitin ligase RNF182 inhibited TLR triggered cytokine production by promoting K48-linked poly-ubiquitination of p65 (Cao, Sun, Chang, Sun, & Yang, 2019). Trim21 promoted K63-linked poly-ubiquitination of p65, but did not affect the stability of p65 (Yang et al., 2021). PDLIM7 cooperated with PDLIM2 to inhibit inflammation by promoting K63-linked poly-ubiquitination of p65 (Jodo et al., 2020). In this study, we revealed that Vangl2 specifically promoted K63-linked poly-ubiquitination of p65, but not other ubiquitin linkages by recruiting a previously unrecognized E3 ligase

PDLIM2, which further explore the molecular mechanism by which regulates the stability of p65.–Although many studies focus on the regulation of p65, the location of p65 degradation has not been clarified. A study showed PDLIM2 degrades p65 through the proteasomal pathway in the nucleus (Jodo et al., 2020), while we found Vangl2 mediated autophagic degradation of p65 mainly happened in cytoplasm, but not in nucleus. Combined with previous studies, our study indicates that p65 undergoes different degradation pathway in distinct location of cells.

Autophagy is a fundamental biological process contributing to multiple life processes. Emerging evidence has suggested that crosstalk between autophagy and innate immune signaling plays critical roles in diseases with inflammatory components, including infections, cancer, autoimmunity, and metabolic disorders (Pradel et al., 2020; Wu et al., 2021). Recent study showed that the interplay between autophagy and type I IFN or NF-κB signaling drives or suppresses inflammatory responses during SARS-CoV-2 infection (Hui et al., 2021). Moreover, autophagy related key genes, such as Atg5, Atg9, and ULK1, also play critical roles in inflammatory diseases (Y. He et al., 2018; Peng et al., 2019). Here, our discovery of Vangl2-PDLIM2-NDP52 complex in the regulation of p65-mediated NF-κB signaling could be a therapeutic target for the development of immunotherapy against infection and inflammation.

The IKK complex plays a pivotal role in the phosphorylation of p65, which in turn influences NF-κB transcriptional activity. Our findings also indicate that Vangl2 deficiency results in an increased accumulation of phosphorylated p65 and IKK also at 30 minutes post-LPS stimulation. However, autophagic degradation of p65 may not have been initiated at this early time point. The function of Vangl2 in mediating NF-κB activation during the early stages of LPS stimulation may be complex. Consequently, these data suggest the intriguing possibility that Vangl2 may also regulate the immediate early phase of the inflammatory response via the IKK-p65 axis, which need further study.

Based on our findings, we propose a working model that Vangl2 negatively regulates NF-κB signaling (Fig. 7 I). Vangl2 functions as an adaptor to recruit ubiquitin ligase PDLIM2 and increase K63-linked ubiquitination on p65, which promotes the recognition of p65 by cargo receptor NDP52 and the autophagic degradation of p65, resulting in suppressing the production of pro-inflammatory cytokines and ameliorating sepsis. Our findings provide a potential target for the treatment of inflammatory diseases.

Materials and Methods

Animal and sepsis model

All animal experiments were approved by the Southern Medical University Animal Care and Use Committee (SMUL20201010). The *Vangl2*$^{flox/flox}$ mice and lysozyme-Cre (*Lyz2*-Cre) mice were obtained from the Jackson Laboratory (Bar Harbor, ME, USA; Jax no. 025174 and 004781, respectively). *Vangl2*$^{flox/flox}$ mice were hybridized with *Lyz2*-Cre mice to obtain *Vangl2*$^{flox/flox}$*Lyz2*-Cre (*Vangl2*$^{\Delta M}$) mice with *Vangl2* specific deficiency in myeloid cells. Co-housed littermate controls with normal *Vangl2* expression were used as wild type (WT). For sepsis model, 10-weeks-old mice were intraperitoneally (i.p.) injected with LPS (25-30 mg/kg), and survival rate of mice was continuously observed. For other detection, mice with sepsis were sacrificed and samples were collected at indicated time points.

Isolation of immune cells

For bone marrow (BM)-derived macrophages (BMDMs), BM cells were collected from the femur and tibia, and then maintained in 20% L929 conditioned media with 1% penicillin-streptomycin and macrophage-colony stimulating factor (M-CSF) (St Louis, MO, USA) for 6 days, as previously described(Tan et al., 2019). Mouse peritoneal macrophages were acquired from ascites of indicated mice, which were administrated intraperitoneally (i.p.) with 4% (v/v) thioglycollate (BD) for three consecutive days before sacrifice. As for primary neutrophils, mice were administrated (i.p.) with 4% (v/v) thioglycollate (BD) for 4 h before sacrifice. Peritoneal cavities were flushed with PBS to obtain peritoneal macrophages or neutrophils. Cells were cultured in complete DMEM (Corning) supplemented with 100 U/ml penicillin (Sigma), 100 μg/ml streptomycin (Sigma) and 10% FBS (HyClone) for 6 h and then washed twice with PBS to remove adherent cells. For human PBMC isolation, 4 ml of whole blood was harvested from each sepsis patient and healthy control. The white membrane layer was collected after density gradient centrifugation at 400 g for 25 min and the PBMCs were filtered and prepared for the subsequent experiments after the removal of the red blood cells. For mouse CD11b^{+} splenocytes isolation, spleens were digested in 2% FBS-DMEM with 200 U/ml DNase I (Sigma, USA) and 1 mg/ml collagenase type II (Sigma, USA) at 37 °C for 30 min. Then tissues digested were filtered through a 70 μm cell strainer and red cells were removed by ACK. The rest splenocytes were labeled with anti-mouse

CD11b biotin antibodies (Biolegend). The mixture above was then incubated with streptavidin-paramagnetic particles (BD Biosciences) at 4 °C for 30 min. Purification of $CD11b^+$ splenocytes was performed by DynaMag™ (Thermo Fisher Science). Isolated cells achieved a purity of ≥95% measured by FACS.

Cell isolation and culture

HEK293T, A549, CHO and Raw 264.7 cells were obtained from the American Type Culture Collection (ATCC). Above cell lines were maintained in complete DMEM, supplemented with 10% FBS, 100 U/ml penicillin and streptomycin. All cells were cultured at 37 °C with 5% CO_2.

Cell treatment

To test cytokines expression and signaling pathway activation, BMDMs, neutrophils and A549 cells were treated with LPS (200 ng/ml) for the indicated time. For dual luciferase assay, HEK293T cells were treated with LPS (250 ng/ml), IL-1β (40 ng/ml) or TNF-α (20 ng/ml) for 6 h. For protein degradation inhibition assays in HEK293T cells, CQ (50 μM), 3MA (10 mM), or bafilomycin A1 (Baf A1) (0.2 μM) was used to inhibit autolysosome- or lysosome-mediated protein degradation. MG132 (10 μM) was used to inhibit proteasome-mediated protein degradation. Z-VAD-FMK (50 μM) was used to inhibit Caspase-mediated protein degradation.

Luciferase and reporter assays

HEK293T cells were plated in 24-well plates and transfected with pRL-TK and plasmids encoding the NF-κB luciferase reporter, together with different plasmids following: Flag-MyD88, Flag-IRAK1, Flag-TRAF6, Flag-IKKα, Flag-IKKβ, Flag-p65 and an increasing doses of the HA-Vangl2 vector (250, 500, 1000 ng) or empty vector. In addition, CHO or HEK293T cells were administrated with or without LPS (1000 ng/ml), IL-1β (1000 ng/ml) or TNF-α (100 ng/ml) for 6-8 h after transfection with pRL-TK and plasmids encoding the NF-κB luciferase reporter. Then, cells were collected at 24 h post-transfection and luciferase activity was analyzed by Dual-Luciferase Reporter Assay Kit (Vazyme) performed with a Luminoskan Ascent luminometer (Thermo Fisher Scientific). The activity of Firefly luciferase was normalized by that of Renilla luciferase to obtain relative luciferase activity.

Enzyme-linked immunosorbent assay (ELISA)

IL-1β, IL-6 and TNF-α in cell supernatants and mice serum were measured using ELISA kit (#E-EL-M0037c, #E-EL-M0044c, #E-EL-M1084c, respectively; Elabscience Biotechnology) following the manufacturer's instructions. Absorbance was detected at 450 nm by the Multiscan FC (Thermo Fisher, Waltham, MA, USA).

Statistical Analysis

The data of all quantitative experiments are presented as mean ± SD of at least three independent experiments. Curve data was assessed by GraphPad Prism 8.0 (USA). And comparisons between groups for statistically significant differences were analyzed with a two-tailed Student's t test. The statistical significance was defined as $p < 0.05$.

Online supplemental material

Fig. S1 shows that the expression of Vangl2 during sepsis and LPS treatment.

Fig. S2 shows that Vangl2 defection promotes LPS-induced NF-κB activation and production of inflammatory cytokines.

Fig. S3 shows that Vangl2 interacts with p65 to inhibit NF-κB activation.

Fig. S4 shows that Vangl2 promotes p65 degradation by autophagic pathway.

Fig. S5 shows that Vangl2 promoted autophagic degradation of p65 is not mediated by cargo receptor p62.

Fig. S6 shows that expression of candidate E3 ubiquitin ligases in WT and Vangl2-deficient BMDMs after LPS treatment.

Table S1 shows reagents and antibodies used in this study.

Table S2 shows primers sequences for quantitative RT-PCR.

Acknowledgments

We thank Dr. Jun Cui (Sun Yat-sen University) for providing ATG5, Beclin1, NDP52, and p62 KO HEK293T cells. We thank Experimental Education/Administration Center of School of Basic Medical Science of Southern Medical University for providing assistance. This work was supported by grants from National Natural Science Foundation of China (82171741, 81801579 and 82302731), Guangdong Basic and Applied Basic Research Foundation (2021A1515012140), and China Postdoctoral Science Foundation (2021M701622).

Author Contributions: J.L., J.Z., H.J. and Z.H. designed and performed the experiments. Y.Z., L.H., D.W., K.Z., P.T., and Z.G. provided assistance or technical support in some experiments. H. L., Y. X., J. Y., Q. X. and Z. S. collected samples. J. L. performed statistical analysis. J.L., J.Z., Z.H., C.P. X.B. and X.Y. performed data analysis and wrote the manuscript. X.Y. supervised the entire project.

References

Ashrafi, G., & Schwarz, T. L. (2013). The pathways of mitophagy for quality control and clearance of mitochondria. *Cell Death Differ, 20*(1), 31-42. doi:10.1038/cdd.2012.81

Bailly, E., Walton, A., & Borg, J. P. (2018). The planar cell polarity Vangl2 protein: From genetics to cellular and molecular functions. *Semin Cell Dev Biol, 81*, 62-70. doi:10.1016/j.semcdb.2017.10.030

Bartuzi, P., Hofker, M. H., & van de Sluis, B. (2013). Tuning NF-kappaB activity: a touch of COMMD proteins. *Biochim Biophys Acta, 1832*(12), 2315-2321. doi:10.1016/j.bbadis.2013.09.014

Brunt, L., Greicius, G., Rogers, S., Evans, B. D., Virshup, D. M., Wedgwood, K. C. A., & Scholpp, S. (2021). Vangl2 promotes the formation of long cytonemes to enable distant Wnt/beta-catenin signaling. *Nat Commun, 12*(1), 2058. doi:10.1038/s41467-021-22393-9

Cancer Genome Atlas Research, N., Kandoth, C., Schultz, N., Cherniack, A. D., Akbani, R., Liu, Y., . . . Levine, D. A. (2013). Integrated genomic characterization of endometrial carcinoma. *Nature, 497*(7447), 67-73. doi:10.1038/nature12113

Cao, Y., Sun, Y., Chang, H., Sun, X., & Yang, S. (2019). The E3 ubiquitin ligase RNF182 inhibits TLR-triggered cytokine production through promoting p65 ubiquitination and degradation. *FEBS Lett, 593*(22), 3210-3219. doi:10.1002/1873-3468.13583

Cartwright, T., Perkins, N. D., & C, L. W. (2016). NFKB1: a suppressor of inflammation, ageing and cancer. *FEBS J, 283*(10), 1812-1822. doi:10.1111/febs.13627

Cerami, E., Gao, J., Dogrusoz, U., Gross, B. E., Sumer, S. O., Aksoy, B. A., . . . Schultz, N. (2012). The cBio cancer genomics portal: an open platform for exploring multidimensional cancer genomics data. *Cancer Discov, 2*(5), 401-404. doi:10.1158/2159-8290.CD-12-0095

Cui, J., Zhu, L., Xia, X., Wang, H. Y., Legras, X., Hong, J., . . . Wang, R. F. (2010). NLRC5 negatively regulates the NF-kappaB and type I interferon signaling pathways. *Cell, 141*(3), 483-496. doi:10.1016/j.cell.2010.03.040

Denton, D., & Kumar, S. (2019). Autophagy-dependent cell death. *Cell Death Differ, 26*(4), 605-616. doi:10.1038/s41418-018-0252-y

Deretic, V. (2021). Autophagy in inflammation, infection, and immunometabolism. *Immunity,*

54(3), 437-453. doi:10.1016/j.immuni.2021.01.018

Feng, D., Wang, J., Yang, W., Li, J. Y., Lin, X. C., Zha, F. Z., . . . Gao, B. (2021). Regulation of Wnt/PCP signaling through p97/VCP-KBTBD7-mediated Vangl ubiquitination and endoplasmic reticulum-associated degradation. *SCIENCE ADVANCES, 7*(20). doi:ARTN eabg2099 10.1126/sciadv.abg2099

Feng, Y., Duan, T., Du, Y., Jin, S., Wang, M., Cui, J., & Wang, R. F. (2017). LRRC25 Functions as an Inhibitor of NF-kappaB Signaling Pathway by Promoting p65/RelA for Autophagic Degradation. *Sci Rep, 7*(1), 13448. doi:10.1038/s41598-017-12573-3

Funes, S. C., Rios, M., Escobar-Vera, J., & Kalergis, A. M. (2018). Implications of macrophage polarization in autoimmunity. *Immunology, 154*(2), 186-195. doi:10.1111/imm.12910

Gao, J., Aksoy, B. A., Dogrusoz, U., Dresdner, G., Gross, B., Sumer, S. O., . . . Schultz, N. (2013). Integrative analysis of complex cancer genomics and clinical profiles using the cBioPortal. *Sci Signal, 6*(269), pl1. doi:10.1126/scisignal.2004088

Gatica, D., Lahiri, V., & Klionsky, D. J. (2018). Cargo recognition and degradation by selective autophagy. *Nat Cell Biol, 20*(3), 233-242. doi:10.1038/s41556-018-0037-z

Gong, Y., Li, Z., Zou, S., Deng, D., Lai, P., Hu, H., . . . Zou, Z. (2021). Vangl2 limits chaperone-mediated autophagy to balance osteogenic differentiation in mesenchymal stem cells. *Dev Cell, 56*(14), 2103-2120 e2109. doi:10.1016/j.devcel.2021.06.011

Hatakeyama, J., Wald, J. H., Printsev, I., Ho, H. Y., & Carraway, K. L., 3rd. (2014). Vangl1 and Vangl2: planar cell polarity components with a developing role in cancer. *Endocr Relat Cancer, 21*(5), R345-356. doi:10.1530/ERC-14-0141

He, X., Zhu, Y., Zhang, Y., Geng, Y., Gong, J., Geng, J., . . . Zhong, H. (2019). RNF34 functions in immunity and selective mitophagy by targeting MAVS for autophagic degradation. *EMBO J, 38*(14), e100978. doi:10.15252/embj.2018100978

He, Y., She, H., Zhang, T., Xu, H., Cheng, L., Yepes, M., . . . Mao, Z. (2018). p38 MAPK inhibits autophagy and promotes microglial inflammatory responses by phosphorylating ULK1. *J Cell Biol, 217*(1), 315-328. doi:10.1083/jcb.201701049

Healy, N. C., & O'Connor, R. (2009). Sequestration of PDLIM2 in the cytoplasm of monocytic/macrophage cells is associated with adhesion and increased nuclear activity of NF-kappaB. *J Leukoc Biol, 85*(3), 481-490. doi:10.1189/jlb.0408238

Hui, X., Zhang, L., Cao, L., Huang, K., Zhao, Y., Zhang, Y., . . . Jin, M. (2021). SARS-CoV-2 promote autophagy to suppress type I interferon response. *Signal Transduct Target Ther, 6*(1), 180. doi:10.1038/s41392-021-00574-8

Jessen, T. N., & Jessen, J. R. (2017). VANGL2 interacts with integrin alphav to regulate matrix metalloproteinase activity and cell adhesion to the extracellular matrix. *Exp Cell Res, 361*(2), 265-276. doi:10.1016/j.yexcr.2017.10.026

Jessen, T. N., & Jessen, J. R. (2019). VANGL2 protein stability is regulated by integrin alphav

and the extracellular matrix. *Exp Cell Res, 374*(1), 128-139. doi:10.1016/j.yexcr.2018.11.017

Jodo, A., Shibazaki, A., Onuma, A., Kaisho, T., & Tanaka, T. (2020). PDLIM7 Synergizes With PDLIM2 and p62/Sqstm1 to Inhibit Inflammatory Signaling by Promoting Degradation of the p65 Subunit of NF-kappaB. *Front Immunol, 11*, 1559. doi:10.3389/fimmu.2020.01559

Johansen, T., & Lamark, T. (2014). Selective autophagy mediated by autophagic adapter proteins. *Autophagy, 7*(3), 279-296. doi:10.4161/auto.7.3.14487

Kauppinen, A., Suuronen, T., Ojala, J., Kaarniranta, K., & Salminen, A. (2013). Antagonistic crosstalk between NF-kappaB and SIRT1 in the regulation of inflammation and metabolic disorders. *Cell Signal, 25*(10), 1939-1948. doi:10.1016/j.cellsig.2013.06.007

Kirkin, V., & Rogov, V. V. (2019). A Diversity of Selective Autophagy Receptors Determines the Specificity of the Autophagy Pathway. *Mol Cell, 76*(2), 268-285. doi:10.1016/j.molcel.2019.09.005

Korbecki, J., Bobinski, R., & Dutka, M. (2019). Self-regulation of the inflammatory response by peroxisome proliferator-activated receptors. *Inflamm Res, 68*(6), 443-458. doi:10.1007/s00011-019-01231-1

Liu, T., Zhang, L., Joo, D., & Sun, S. C. (2017). NF-kappaB signaling in inflammation. *Signal Transduct Target Ther, 2*. doi:10.1038/sigtrans.2017.23

Locati, M., Curtale, G., & Mantovani, A. (2020). Diversity, Mechanisms, and Significance of Macrophage Plasticity. *Annu Rev Pathol, 15*, 123-147. doi:10.1146/annurev-pathmechdis-012418-012718

Mao, X., Gluck, N., Li, D., Maine, G. N., Li, H., Zaidi, I. W., . . . Burstein, E. (2009). GCN5 is a required cofactor for a ubiquitin ligase that targets NF-kappaB/RelA. *Genes Dev, 23*(7), 849-861. doi:10.1101/gad.1748409

Mitxitorena, I., Somma, D., Mitchell, J. P., Lepisto, M., Tyrchan, C., Smith, E. L., . . . Carmody, R. J. (2020). The deubiquitinase USP7 uses a distinct ubiquitin-like domain to deubiquitinate NF-kB subunits. *J Biol Chem, 295*(33), 11754-11763. doi:10.1074/jbc.RA120.014113

Nagaoka, T., Furuse, M., Ohtsuka, T., Tsuchida, K., & Kishi, M. (2019). Vangl2 interaction plays a role in the proteasomal degradation of Prickle2. *Sci Rep, 9*(1), 2912. doi:10.1038/s41598-019-39642-z

Otten, E. G., Werner, E., Crespillo-Casado, A., Boyle, K. B., Dharamdasani, V., Pathe, C., . . . Randow, F. (2021). Ubiquitylation of lipopolysaccharide by RNF213 during bacterial infection. *Nature, 594*(7861), 111-116. doi:10.1038/s41586-021-03566-4

Papakrivopoulou, E., Vasilopoulou, E., Lindenmeyer, M. T., Pacheco, S., Brzoska, H. L., Price, K. L., . . . Long, D. A. (2018). Vangl2, a planar cell polarity molecule, is implicated in irreversible and reversible kidney glomerular injury. *J Pathol, 246*(4), 485-496. doi:10.1002/path.5158

Peng, X., Wang, Y., Li, H., Fan, J., Shen, J., Yu, X., . . . Mao, H. (2019). ATG5-mediated autophagy suppresses NF-kappaB signaling to limit epithelial inflammatory response to kidney injury. *Cell Death Dis, 10*(4), 253. doi:10.1038/s41419-019-1483-7

Poobalasingam, T., Yates, L. L., Walker, S. A., Pereira, M., Gross, N. Y., Ali, A., . . . Dean, C. H. (2017). Heterozygous Vangl2(Looptail) mice reveal novel roles for the planar cell polarity pathway in adult lung homeostasis and repair. *Dis Model Mech, 10*(4), 409-423. doi:10.1242/dmm.028175

Pradel, B., Robert-Hebmann, V., & Espert, L. (2020). Regulation of Innate Immune Responses by Autophagy: A Goldmine for Viruses. *Front Immunol, 11*, 578038. doi:10.3389/fimmu.2020.578038

Puvirajesinghe, T. M., Bertucci, F., Jain, A., Scerbo, P., Belotti, E., Audebert, S., . . . Borg, J. P. (2016). Identification of p62/SQSTM1 as a component of non-canonical Wnt VANGL2-JNK signalling in breast cancer. *Nat Commun, 7*, 10318. doi:10.1038/ncomms10318

Shaid, S., Brandts, C. H., Serve, H., & Dikic, I. (2013). Ubiquitination and selective autophagy. *Cell Death Differ, 20*(1), 21-30. doi:10.1038/cdd.2012.72

Tan, P., He, L., Xing, C., Mao, J., Yu, X., Zhu, M., . . . Wang, R. F. (2019). Myeloid loss of Beclin 1 promotes PD-L1hi precursor B cell lymphoma development. *J Clin Invest, 129*(12), 5261-5277. doi:10.1172/JCI127721

Tong, Y., Cui, J., Li, Q., Zou, J., Wang, H. Y., & Wang, R. F. (2012). Enhanced TLR-induced NF-kappaB signaling and type I interferon responses in NLRC5 deficient mice. *Cell Res, 22*(5), 822-835. doi:10.1038/cr.2012.53

Wu, Y., Jin, S., Liu, Q., Zhang, Y., Ma, L., Zhao, Z., . . . Cui, J. (2021). Selective autophagy controls the stability of transcription factor IRF3 to balance type I interferon production and immune suppression. *Autophagy, 17*(6), 1379-1392. doi:10.1080/15548627.2020.1761653

Yamano, K., & Youle, R. J. (2020). Two different axes CALCOCO2-RB1CC1 and OPTN-ATG9A initiate PRKN-mediated mitophagy. *Autophagy, 16*(11), 2105-2107. doi:10.1080/15548627.2020.1815457

Yang, L., Zhang, T., Zhang, C., Xiao, C., Bai, X., & Wang, G. (2021). Upregulated E3 ligase tripartite motif-containing protein 21 in psoriatic epidermis ubiquitylates nuclear factor-kappaB p65 subunit and promotes inflammation in keratinocytes. *Br J Dermatol, 184*(1), 111-122. doi:10.1111/bjd.19057

Yin, Z., Popelka, H., Lei, Y., Yang, Y., & Klionsky, D. J. (2020). The Roles of Ubiquitin in Mediating Autophagy. *Cells, 9*(9). doi:10.3390/cells9092025

Figure legends

Figure 1. Vangl2 ablation promotes inflammation during LPS treatment.

(A) Transcription levels of *Vangl2* in PBMCs from healthy volunteers (healthy control, HC) and sepsis patients were analyzed by real-time PCR (n=8).

(B) *Vangl2* mRNA in different organs from mice treated with or without LPS (n≥3).

(C) The survival rates of WT and *Vangl2*$^{\Delta M}$ mice treated with high-dosage of LPS (30 mg/kg, i.p.) (n≥4).

(D-F) WT and *Vangl2*$^{\Delta M}$ mice (n≥3) were treated with LPS (30 mg/kg, i.p.). Splenocytes were collected at 9 h after LPS treatment. Cell lysates of CD11b^{+} sorted splenocytes were analyzed by immunoblotting with the indicated antibodies **(D)**. RNAs from splenocytes were isolated and used for expression analysis of *Il1b*, *Tnfa*, and *Il6* using qPCR **(E)**. Sera were collected at indicated times post LPS treatment and subjected to ELISA analysis of IL-1β, TNF-α, and IL-6 **(F)**.

PBMCs, peripheral blood mononuclear cells; Unsti, unstimulation; LPS, lipopolysaccharide; LN, lymph node; SP, spleen. Data are representative of three independent experiments and are plotted as the mean ±SD. **p*<0.05, ***p*<0.01, ****p*<0.001 vs. corresponding control.

Figure 2. Vangl2 negatively regulates LPS-induced NF-κB activation and proinflammatory cytokines.

(A-D) WT and Vangl2-deficient (n≥3) pMAC **(A and C)** or neutrophils **(B and D)** were stimulated with LPS (100 ng/ml) for the indicated times. Immunoblot analysis of total and phosphorylated p65, IKKα/β **(A and B)**, and analysis of grey intensity was shown **(C and D)**.

(E-F) WT and Vangl2-deficient (n≥4) pMAC or neutrophils were stimulated with LPS (100 ng/ml) for 6 h. mRNA levels of *Il6* and *Tnfa* were measure by qPCR **(E)**. IL-6 and TNF-α secretion by WT and Vangl2-deficient BMDMs or neutrophils treated with or without LPS for 6 h was measured by ELISA **(F)**.

(G and H) The WT and Vangl2-deficient (n≥3) neutrophils were treated with LPS (1000 ng/ml) for 4 h, and the nuclear translocation of p65 was detected by immunofluorescence **(G)** (p65, green; DAPI, blue; Scale bar, 50 μm). Percentages of

p65 nuclear translocated cells in WT and Vangl2-deficient neutrophils were determined by counting 100 to 150 cells in non-overlapping fields **(H)**.

(I and J) A549 cells were transfected with Flag-tagged Vangl2 plasmid or empty vector, then stimulated with LPS (100 ng/ml) for the indicated times. Immunoblot analysis of total and phosphorylated p65, IKKα/β **(I)** (representative image), and analysis of grey intensity was shown **(J)** (n≥3).

pMAC, peritoneal macrophage; Neu, neutrophil; EV, empty vector. Data are representative of three independent experiments and are plotted as the mean ±SD. **p*<0.05, ***p*<0.01, ****p*<0.001 vs. corresponding control.

Figure 3. Vangl2 inhibits NF-κB signaling by interacting with p65.

(A-C) Cho **(A)** or HEK293T cells **(B and C)** were co-transfected with a NF-κB and TK-Renilla reporter along with increasing amounts of Vangl2 for 18 h, then treated the cells with or without LPS (A, 250 ng/ml), IL-1β (B, 40 ng/ml), or TNF-α (C, 20 ng/ml) for 6 h. NF-κB promoter driven luciferase activity was measured and normalized to the Renilla luciferase activity.

(D) Luciferase activity in HEK293T transfected with plasmids encoding an NF-κB luciferase reporter and TK-Renilla reporter, together with a vector encoding MyD88, IRAK1, TRAF6, IKKα, IKKβ, or p65, along with or without Vangl2 plasmid, was measured at 24 h after transfection and normalized to the Renilla luciferase activity.

(E) HEK293T cells were transfected with plasmids encoding HA-tagged Vangl2 and Flag-tagged p65, followed by immunoprecipitation with anti-Flag beads and immunoblot analysis with anti-HA. Throughout was the immunoblot analysis of whole-cell lysates without immunoprecipitation.

(F) BMDMs were stimulated with LPS (100 ng/ml) for the indicated times. The cell lysates were subjected to immunoprecipitation with an anti-p65 antibody or control IgG, followed by immunoblotting with indicated antibodies.

(G) The WT and Vangl2-deficient peritoneal macrophages were treated with LPS (1000 ng/ml) for 4 h, and co-localization of p65 and Vangl2 was detected by immunofluorescence (p65, green; Vangl2, red; DAPI, blue; Scale bar, 50 μm).

(H) A structural diagram of Vangl2 as well as schematic representation of Myc-tagged truncation mutants of Vangl2 (top). HEK293T cells were transfected with Flag-tagged p65 and empty vector, Myc-tagged Vangl2 (FL) or Vangl2 truncation mutants. The cell

lysates were subjected to immunoprecipitation with anti-Flag beads and immunoblotted with the indicated antibodies (bottom).

(I) HEK293T cells were transfected with Flag-tagged p65 and HA-tagged Vangl2 FL or PkBD truncation. The cell lysates were subjected to immunoprecipitation with anti-Flag beads and immunoblotted with the indicated antibodies.

(J) Luciferase activity in HEK293T cells transfected with an NF-κB luciferase reporter, together with a vector encoding p65, along with the empty vector or with vectors encoding Vangl2 or its truncation mutants. The results are presented relative to Renilla luciferase activity.

IP, immunoprecipitation; WCL, whole-cell lysate. Data are representative of three independent experiments and are plotted as the mean ±SD. *p<0.05, **p<0.01, ***p<0.001 vs. corresponding control. NS, not significant.

Figure 4. Vangl2 promotes the autophagic degradation of p65.

(A) Immunoblot analysis of HEK293T cells transfected with Flag-p65 and increasing amounts of the vector encoding HA-Vangl2 (0, 250, 500, and 1000 ng).

(B) Total RNA from HEK293T cells as in (A) was isolated and measured by semi-quantitative PCR.

(C) HEK293T cells transfected with Flag-p65 and increasing amounts of the vector encoding HA-Vangl2, and the expressions of p65 in nuclear or cytoplasm were detected by immunoblot.

(D) WT and Vangl2-deficient BMDMs were treated with LPS for the indicated times, and the expressions of p65 and Vangl2 were detected by immunoblot.

(E) HEK293T cells were transfected with Flag-p65 and HA-Vangl2 plasmids, and treated with DMSO, MG132 (10 μM), CQ (50 μM), 3-MA (10 mM) or Baf-A1 (0.2 μM) for 6 h. The cell lysates were analyzed by immunoblot.

(F) HEK293T cells were transfected with empty vector (EV) or Flag-Vangl2 plasmid, and treated with rapamycin for the indicated times. The cell lysates were analyzed by immunoblot with indicated antibodies.

(G) WT, ATG5 KO and Beclin1 KO HEK293T cells were transfected with Flag-p65, together with or without HA-Vangl2 plasmids, and then the cell lysates were analyzed by immunoblot with indicated antibodies.

(H and I) Luciferase activity in WT, ATG5 KO **(G)** and Beclin1 KO **(H)** HEK293T cells transfected with plasmids encoding an NF-κB luciferase reporter and TK-Renilla reporter, together with p65 plasmid along with increasing amounts of Vangl2, was measured at 24 h after transfection and normalized to the Renilla luciferase activity.

CHX, cycloheximide; 3-MA, 3-methyladenine; CQ, chloroquine; Baf A1, bafilomycin A1. Data are representative of three independent experiments and are plotted as the mean ±SD. *p<0.05, **p<0.01, ***p<0.001 vs. corresponding control. NS, not significant.

Figure 5. Vangl2 enhances the recognition of p65 by cargo receptor NDP52.

(A) HEK293T cells transfected with a vector expressing HA-Vangl2 along with the empty vector or vector encoding Flag-p62/NDP52/NBR1/Nix. The cell lysates were subjected to immunoprecipitation with anti-Flag beads and immunoblotted with the indicated antibodies.

(B) HEK293T cells transfected with a vector expressing HA-p65 along with the empty vector or vector encoding Flag-p62/NDP52/NBR1/Nix. The cell lysates were subjected to immuno-precipitation with anti-Flag beads and immunoblotted with the indicated antibodies.

(C) HEK293T cells were transfected with HA-p65 together with Flag-NDP52 or Flag-p62, as well as with empty vector or Myc-Vangl2. The cell lysates were subjected to immunoprecipitation with anti-Flag beads and immunoblotted with the indicated antibodies.

(D) WT, NDP52 KO and p62 KO HEK293T cells were transfected with a vector expressing HA-p65 along with the empty vector or vector encoding Flag-Vangl2. The cell lysates were immunoblotted with the indicated antibodies.

(E) WT and Vangl2-deficient BMDMs were stimulated with LPS (100 ng/ml) for the indicated times. The cell lysates were subjected to immunoprecipitation with an anti-p65 antibody or control IgG and immunoblotted with the indicated antibodies.

(F) WT and NDP52 KO HEK293T cells were transfected with a vector expressing HA-p65 along with the empty vector or vector encoding Flag-Vangl2. The cell lysates were subjected to immunoprecipitation with anti-Flag beads and immunoblotted with the indicated antibodies.

(G) Luciferase activity in WT and NDP52 KO HEK293T cells transfected with plasmids encoding NF-κB luciferase reporter and TK-Renilla reporter, together with p65 plasmid

along with increasing amounts of Vangl2 plasmid, was measured at 24 h after transfection.

(H) WT and NDP52 KO HEK293T were treated with CHX for the indicated times. The cell lysates were immunoblotted with the indicated antibodies.

Data are representative of three independent experiments and are plotted as the mean ±SD. *p<0.05, **p<0.01, ***p<0.001 vs. corresponding control. NS, not significant.

Figure 6. Vangl2 increases the K63-linked ubiquitination of p65.

(A) WT and Vangl2-deficient BMDMs were stimulated with LPS (100 ng/ml) for the indicated times. The cell lysates were subjected to immunoprecipitation with an anti-p65 antibody or control IgG and immunoblotted with the indicated antibodies.

(B) HEK293T cells were transfected with Flag-p65, Myc-Vangl2, HA-Ub or HA-K63 plasmids with the indicated combinations for 24 h and then treated with CQ for 8 h. The cell lysates were subjected to immunoprecipitation with anti-Flag beads and immunoblotted with the indicated antibodies.

(C) HEK293T cells were transfected with Flag-p65, Myc-Vangl2 and HA-Ub/K63/K11/K27/K33/K48 plasmids with the indicated combinations for 24 h and then treated with CQ and Baf-A1 for 8 h. The cell lysates were subjected to immunoprecipitation with anti-Flag beads and immunoblotted with the indicated antibodies.

(D) HEK293T cells were transfected with a vector expressing Flag-p65 and HA-K63 along with *Scramble* or *Vangl2* siRNA. The cell lysates were subjected to immunoprecipitation with anti-Flag beads and immunoblotted with the indicated antibodies.

Data are representative of three independent experiments.

Figure 7. Vangl2 recruits PDLIM2 to ubiquitinate p65.

(A) HEK293T cells were transfected with the indicated siRNA, NF-κB reporter plasmids together with HA-Vangl2, Flag-p65 or the control vector as indicated for 24 h, and then subjected to luciferase assay and immunoblotting analysis.

(B and C) BMDMs were transfected with *Pdlim2* or *Scramble* siRNA along with the empty vector or vector encoding Flag-Vangl2, stimulated with LPS (100 ng/ml) for 6 h, then analyzed by qPCR for *Il6* **(B)** and *Il1b* **(C)** expression.

(D) HEK293T cells transfected with HA- PDLIM2 along with the empty vector or vector encoding Flag-Vangl2. The cell lysates were subjected to immunoprecipitation with anti-Flag beads and immunoblotted with the indicated antibodies.

(E) HEK293T cells were transfected with Flag-p65, HA-PDLIM2 and Myc-Vangl2 plasmids with the indicated combinations for 24 h and then treated with CQ and Baf-A1 for 8 h. The cell lysates were subjected to immunoprecipitation with anti-Flag beads and immunoblotted with the indicated antibodies.

(F) HEK293T cells were transfected with Flag-p65, HA-PDLIM2 and Myc-Vangl2 plasmids with the indicated combinations for 24 h. The cell lysates were immunoblotted with the indicated antibodies.

(G) HEK293T cells were transfected with Flag-p65, HA-K63 and Myc-Vangl2 plasmids, the expression of E3 ubiquitin ligase was interfered with *Pdlim2* siRNA and then treated with CQ and Baf-A1 for 8 h. The cell lysates were subjected to immunoprecipitation with anti-Flag beads and immunoblotted with the indicated antibodies.

(H) HEK293T cells were transfected with *Pdlim2* or *Scramble* siRNA, along with or without HA-PDLIM2, then treated with CQ and Baf-A1 for 8 h. The cell lysates were subjected to immunoprecipitation with anti-Flag beads and immunoblotted with the indicated antibodies.

(I) A schematic model to illustrate how Vangl2-PDLIM2-NDP52-p65 axis negatively regulates NF-κB activation. During LPS stimulation, Vangl2 expression is up-regulated, thus constituting a negative feedback loop to regulate NF-κB activation. In detail, Vangl2 functions as an adaptor protein to recruit an E3 ubiquitin ligase PDLIM2 to increase K63-linked ubiquitination of p65 and promotes NDP52-mediated p65 degradation through selective autophagy, resulting in ameliorating sepsis and suppressing production of pro-inflammatory cytokines.

Data are representative of three independent experiments and are plotted as the mean ±SD. *p<0.05, **p<0.01, ***p<0.001 vs. corresponding control. NS, not significant.

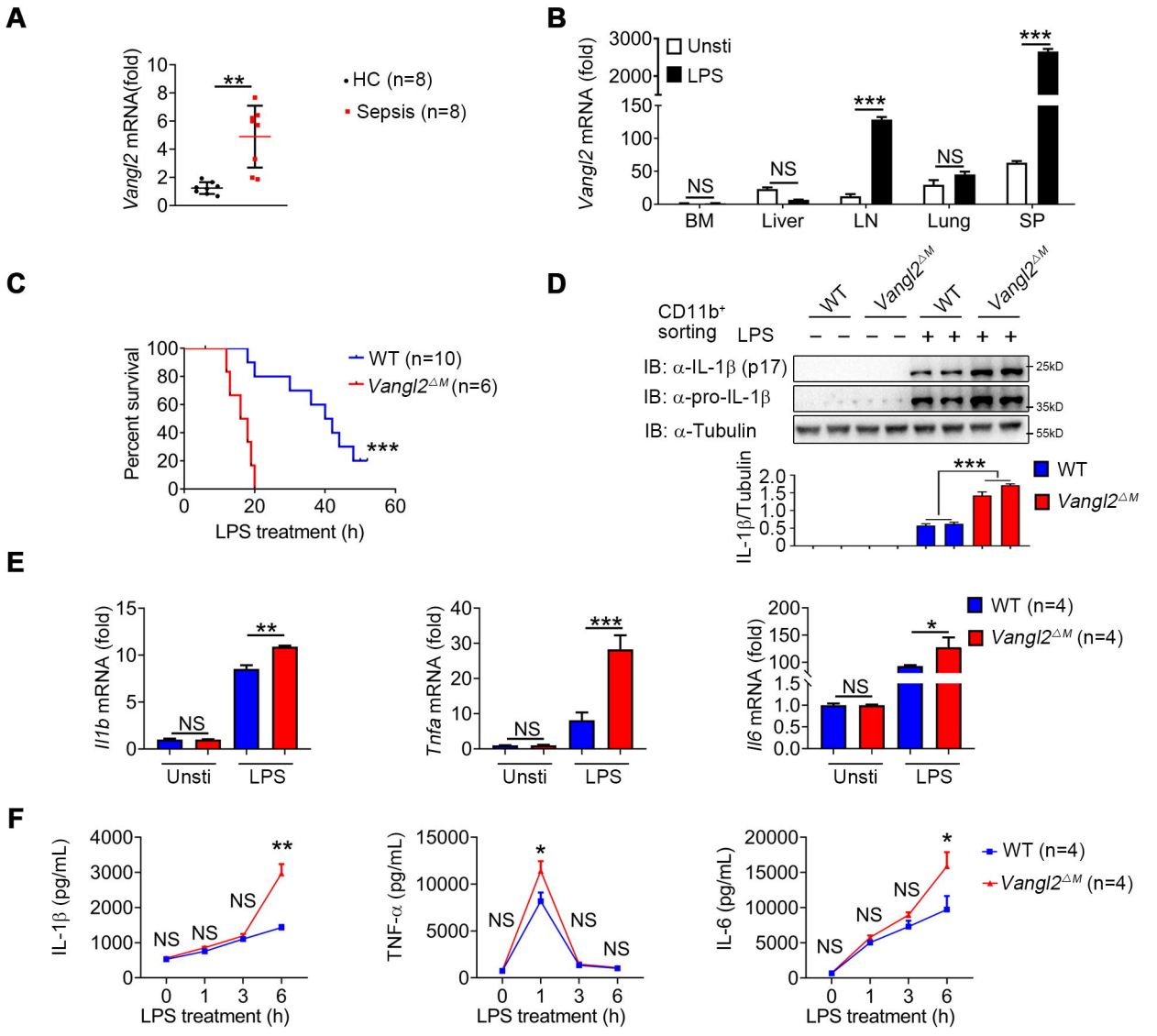
A
Vangl2 mRNA(fold)
10
8
6
4
2
0
**
HC (n=8)
Sepsis (n=8)
B
Vangl2 mRNA (fold)
3000
2000
150
100
50
0
Unsti
LPS
NS
NS
***
NS
***
BM
Liver
LN
Lung
SP
C
Percent survival
100
80
60
40
20
0
0
20
40
60
LPS treatment (h)
WT (n=10)
Vangl2ΔM (n=6)
***
D
CD11b+ sorting
WT
Vangl2ΔM
WT
Vangl2ΔM
LPS
– – – – + + + +
IB: α-IL-1β (p17)
IB: α-pro-IL-1β
IB: α-Tubulin
25kD
35kD
55kD
IL-1β/Tubulin
2.0
1.5
1.0
0.5
0
***
WT
Vangl2ΔM
E
Il1b mRNA (fold)
15
10
5
0
NS
**
Unsti
LPS
Tnfa mRNA (fold)
40
30
20
10
0
NS
***
Unsti
LPS
Il6 mRNA (fold)
200
150
100
1.5
1.0
0.5
0.0
NS
*
Unsti
LPS
WT (n=4)
Vangl2ΔM (n=4)
F
IL-1β (pg/mL)
4000
3000
2000
1000
0
NS
NS
NS
**
0
1
3
6
LPS treatment (h)
TNF-α (pg/mL)
15000
10000
5000
0
NS
*
NS
NS
0
1
3
6
LPS treatment (h)
IL-6 (pg/mL)
20000
15000
10000
5000
0
NS
NS
NS
*
0
1
3
6
LPS treatment (h)
WT (n=4)
Vangl2ΔM (n=4)

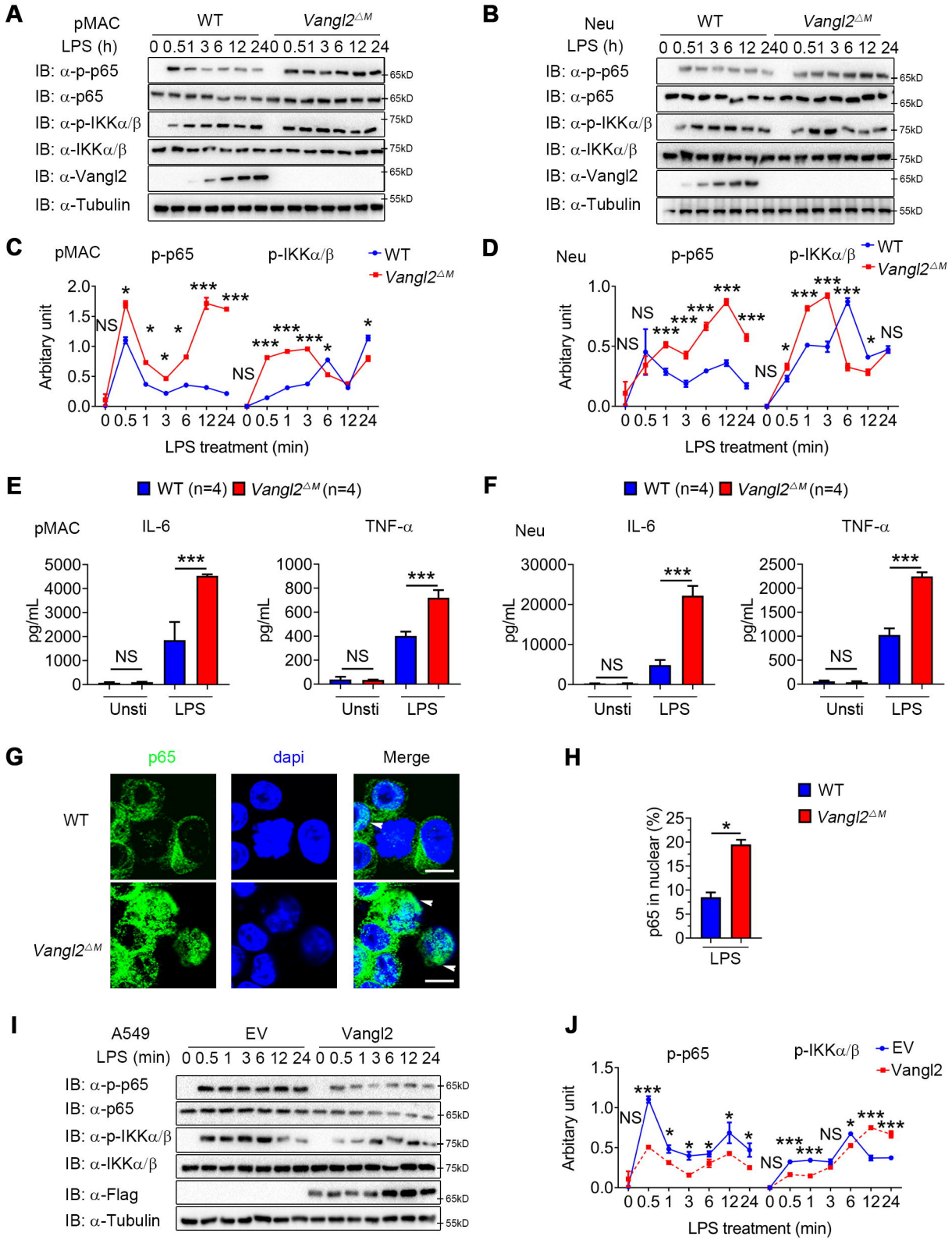
A
pMAC
WT
Vangl2△M
LPS (h)
0 0.51 3 6 12 24 0 0.51 3 6 12 24
IB: α-p-p65
IB: α-p65
IB: α-p-IKKα/β
IB: α-IKKα/β
IB: α-Vangl2
IB: α-Tubulin
65kD
75kD
55kD
B
Neu
WT
Vangl2△M
LPS (h)
0 0.51 3 6 12 24 0 0.51 3 6 12 24
IB: α-p-p65
IB: α-p65
IB: α-p-IKKα/β
IB: α-IKKα/β
IB: α-Vangl2
IB: α-Tubulin
C
pMAC
p-p65
p-IKKα/β
WT
Vangl2△M
Arbitary unit
LPS treatment (min)
D
Neu
p-p65
p-IKKα/β
WT
Vangl2△M
Arbitary unit
LPS treatment (min)
E
WT (n=4) Vangl2△M (n=4)
pMAC
IL-6
TNF-α
pg/mL
Unsti
LPS
F
WT (n=4) Vangl2△M (n=4)
Neu
IL-6
TNF-α
pg/mL
Unsti
LPS
G
p65
dapi
Merge
WT
Vangl2△M
H
WT
Vangl2△M
p65 in nuclear (%)
LPS
I
A549
EV
Vangl2
LPS (min)
0 0.5 1 3 6 12 24 0 0.5 1 3 6 12 24
IB: α-p-p65
IB: α-p65
IB: α-p-IKKα/β
IB: α-IKKα/β
IB: α-Flag
IB: α-Tubulin
J
p-p65
p-IKKα/β
EV
Vangl2
Arbitary unit
LPS treatment (min)

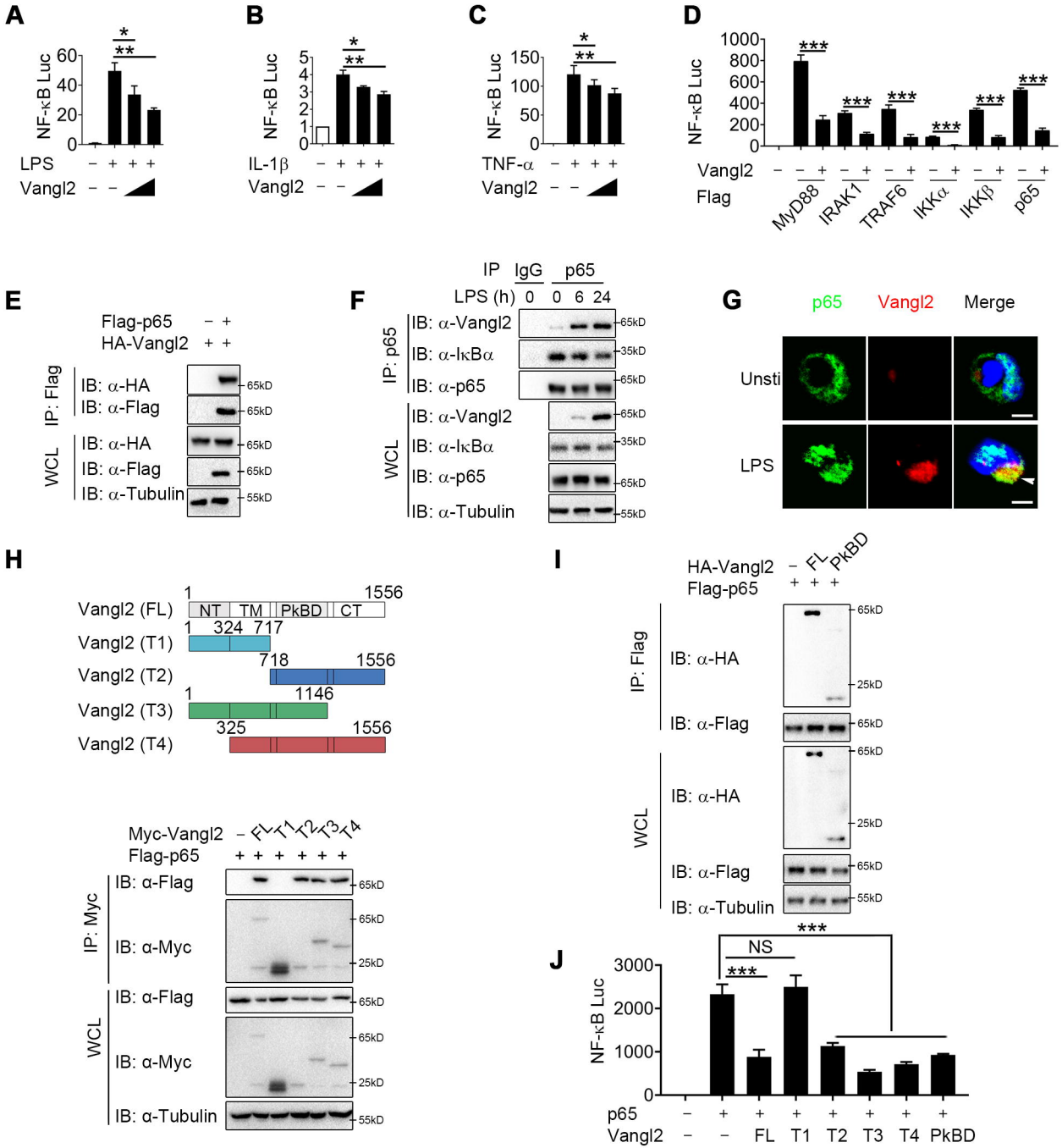
A
NF-κB Luc
LPS
Vangl2
B
NF-κB Luc
IL-1β
Vangl2
C
NF-κB Luc
TNF-α
Vangl2
D
NF-κB Luc
Vangl2
Flag
MyD88
IRAK1
TRAF6
IKKα
IKKβ
p65
E
Flag-p65
HA-Vangl2
IP: Flag
IB: α-HA
IB: α-Flag
WCL
IB: α-HA
IB: α-Flag
IB: α-Tubulin
65kD
55kD
F
IP
IgG
p65
LPS (h)
IP: p65
IB: α-Vangl2
IB: α-IκBα
IB: α-p65
WCL
IB: α-Vangl2
IB: α-IκBα
IB: α-p65
IB: α-Tubulin
65kD
35kD
55kD
G
p65
Vangl2
Merge
Unsti
LPS
H
Vangl2 (FL)
NT
TM
PkBD
CT
Vangl2 (T1)
Vangl2 (T2)
Vangl2 (T3)
Vangl2 (T4)
Myc-Vangl2
Flag-p65
IP: Myc
IB: α-Flag
IB: α-Myc
WCL
IB: α-Flag
IB: α-Myc
IB: α-Tubulin
65kD
25kD
55kD
I
HA-Vangl2
Flag-p65
FL
PkBD
IP: Flag
IB: α-HA
IB: α-Flag
WCL
IB: α-HA
IB: α-Flag
IB: α-Tubulin
65kD
25kD
55kD
J
NF-κB Luc
NS
p65
Vangl2
FL
T1
T2
T3
T4
PkBD

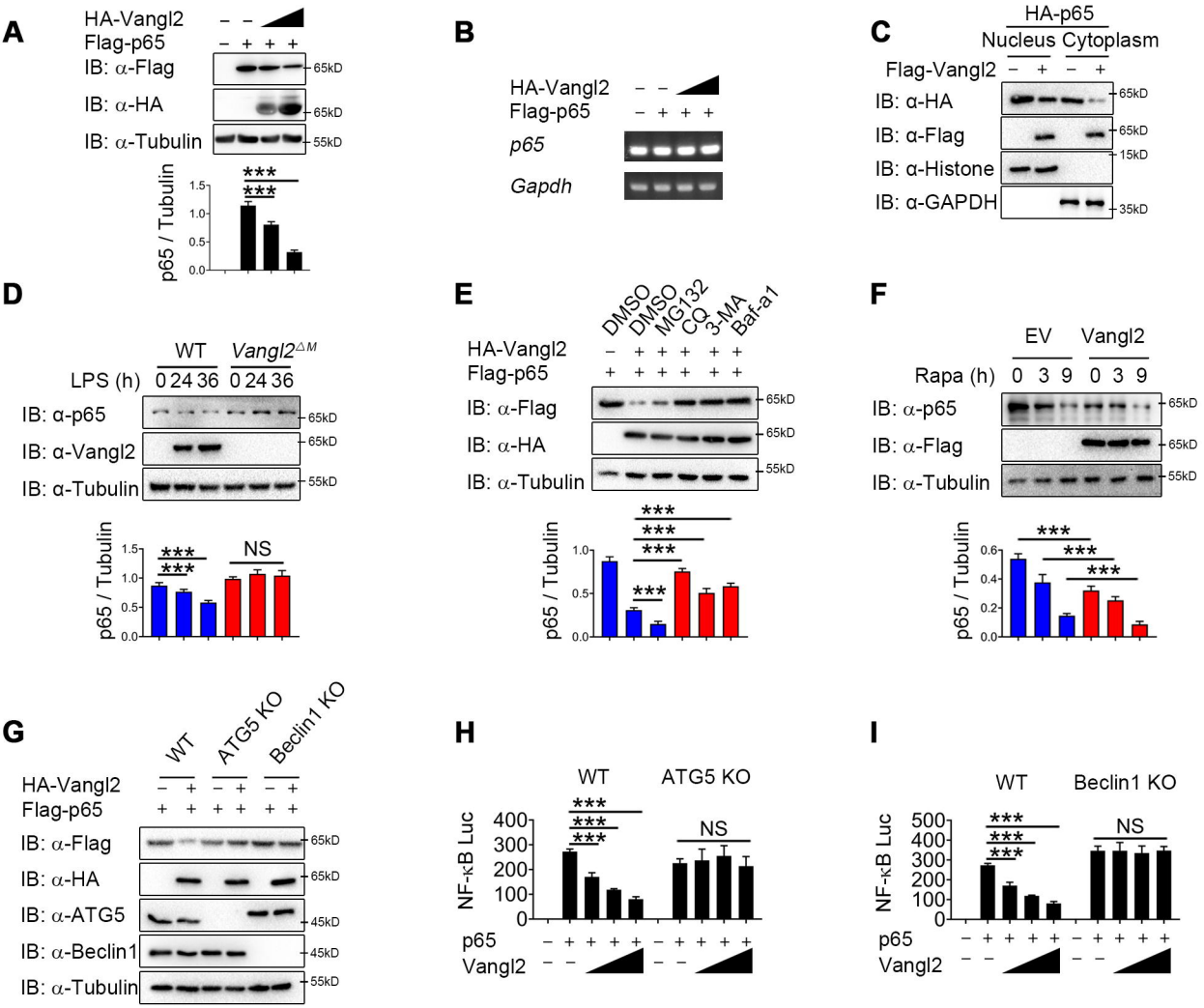
A
HA-Vangl2
Flag-p65
IB: α-Flag
IB: α-HA
IB: α-Tubulin
65kD
55kD
p65 / Tubulin
B
HA-Vangl2
Flag-p65
p65
Gapdh
C
HA-p65
Nucleus Cytoplasm
Flag-Vangl2
IB: α-HA
IB: α-Flag
IB: α-Histone
IB: α-GAPDH
15kD
35kD
D
WT
Vangl2ΔM
LPS (h)
0 24 36 0 24 36
IB: α-p65
IB: α-Vangl2
NS
E
DMSO
DMSO
MG132
CQ
3-MA
Baf-a1
F
EV
Vangl2
Rapa (h)
0 3 9 0 3 9
G
WT
ATG5 KO
Beclin1 KO
IB: α-ATG5
IB: α-Beclin1
45kD
H
NF-κB Luc
p65
Vangl2
I

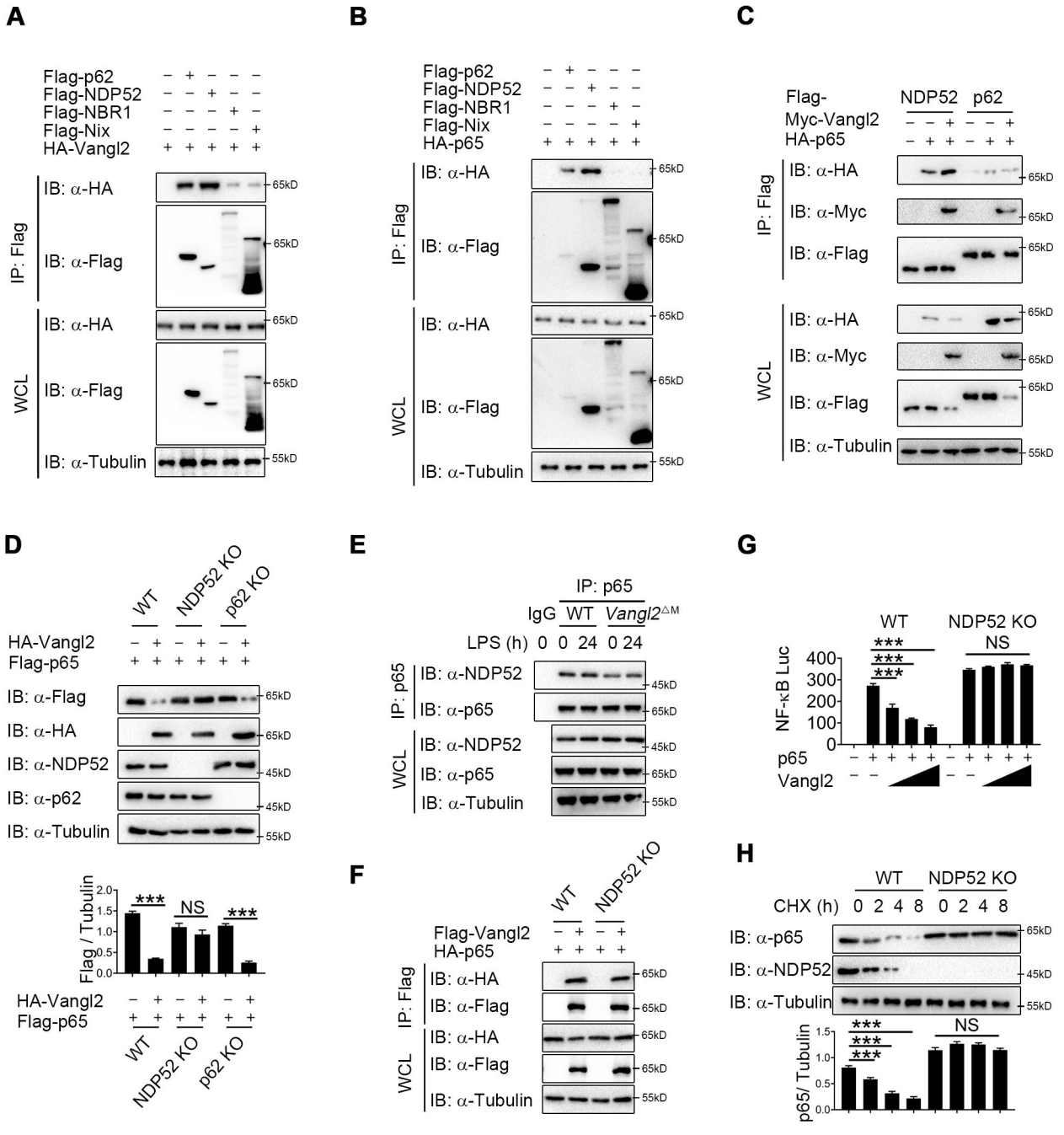
A
Flag-p62
Flag-NDP52
Flag-NBR1
Flag-Nix
HA-Vangl2
IP: Flag
WCL
IB: α-HA
IB: α-Flag
IB: α-Tubulin
65kD
55kD
B
Flag-p62
Flag-NDP52
Flag-NBR1
Flag-Nix
HA-p65
C
Flag-
Myc-Vangl2
HA-p65
NDP52
p62
IB: α-Myc
D
WT
NDP52 KO
p62 KO
HA-Vangl2
Flag-p65
IB: α-NDP52
IB: α-p62
Flag / Tubulin
***
NS
E
IP: p65
IgG
WT
Vangl2△M
LPS (h) 0 0 24 0 24
IP: p65
45kD
F
G
NF-κB Luc
p65
Vangl2
H
CHX (h) 0 2 4 8 0 2 4 8
p65/ Tubulin

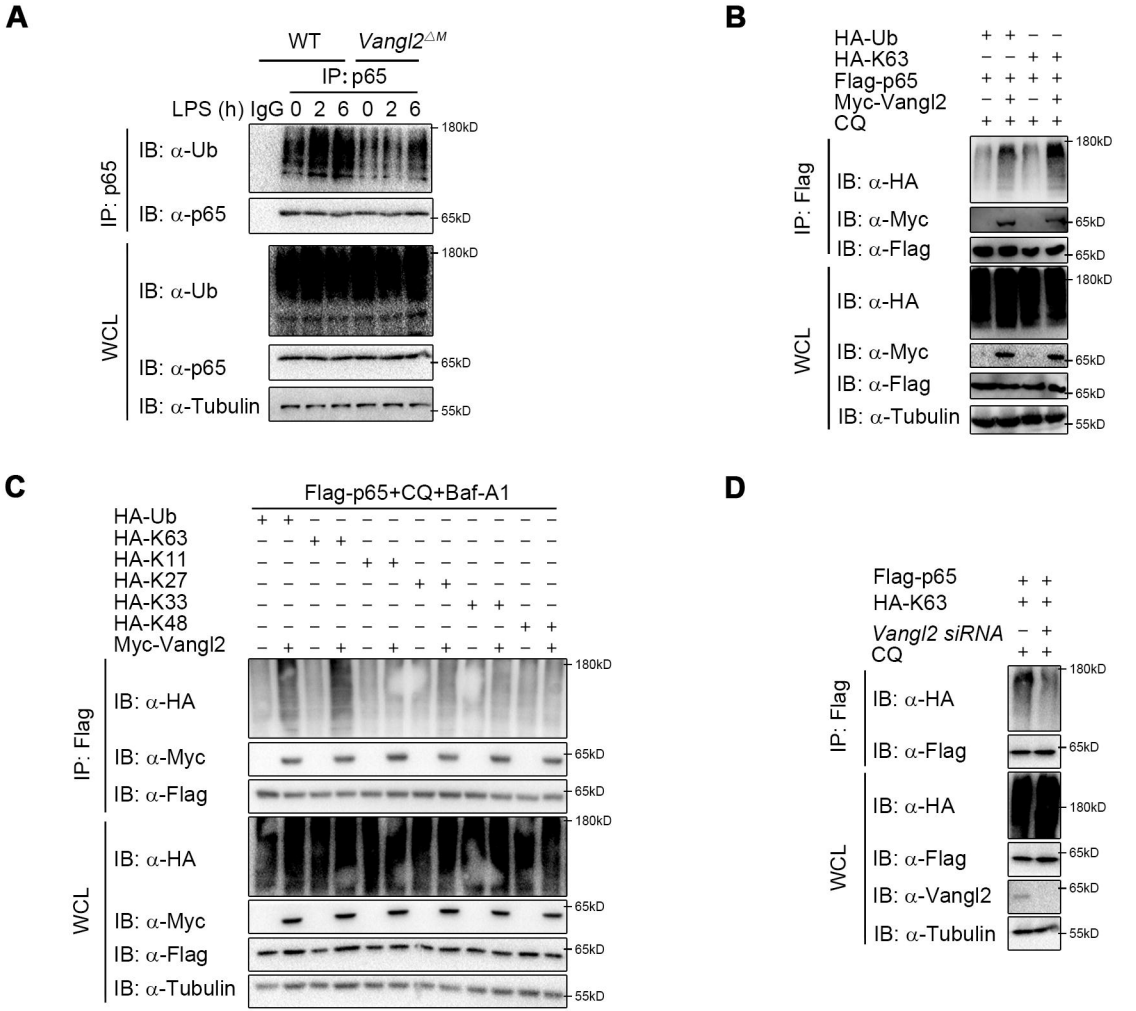
A
WT
Vangl2△M
IP: p65
LPS (h) IgG 0 2 6 0 2 6
IP: p65
IB: α-Ub
IB: α-p65
WCL
IB: α-Ub
IB: α-p65
IB: α-Tubulin
180kD
65kD
180kD
65kD
55kD
B
HA-Ub + + − −
HA-K63 − − + +
Flag-p65 + + + +
Myc-Vangl2 − + − +
CQ + + + +
IP: Flag
IB: α-HA
IB: α-Myc
IB: α-Flag
WCL
IB: α-HA
IB: α-Myc
IB: α-Flag
IB: α-Tubulin
180kD
65kD
65kD
180kD
65kD
65kD
55kD
C
Flag-p65+CQ+Baf-A1
HA-Ub + + − − − − − − − − − −
HA-K63 − − + + − − − − − − − −
HA-K11 − − − − + + − − − − − −
HA-K27 − − − − − − + + − − − −
HA-K33 − − − − − − − − + + − −
HA-K48 − − − − − − − − − − + +
Myc-Vangl2 − + − + − + − + − + − +
IP: Flag
IB: α-HA
IB: α-Myc
IB: α-Flag
WCL
IB: α-HA
IB: α-Myc
IB: α-Flag
IB: α-Tubulin
180kD
65kD
65kD
180kD
65kD
65kD
55kD
D
Flag-p65 + +
HA-K63 + +
Vangl2 siRNA − +
CQ + +
IP: Flag
IB: α-HA
IB: α-Flag
WCL
IB: α-HA
IB: α-Flag
IB: α-Vangl2
IB: α-Tubulin
180kD
65kD
180kD
65kD
65kD
55kD

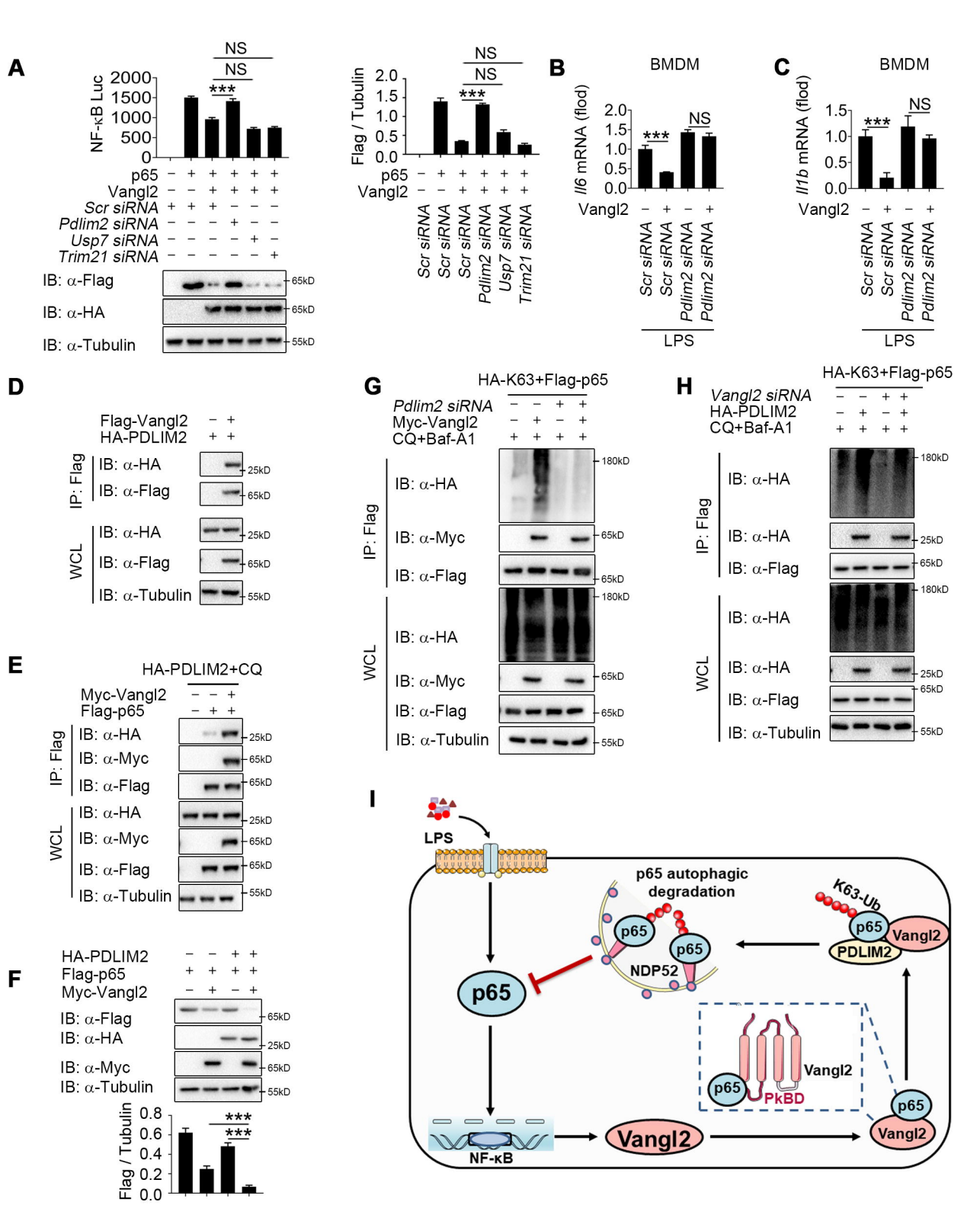
A
NF-κB Luc
2000
1500
1000
500
0
NS
NS
***
p65
Vangl2
Scr siRNA
Pdlim2 siRNA
Usp7 siRNA
Trim21 siRNA
IB: α-Flag
IB: α-HA
IB: α-Tubulin
65kD
55kD
Flag / Tubulin
2.0
1.5
1.0
0.5
0.0
B
BMDM
Il6 mRNA (flod)
Vangl2
LPS
C
BMDM
Il1b mRNA (flod)
D
Flag-Vangl2
HA-PDLIM2
IP: Flag
WCL
25kD
E
HA-PDLIM2+CQ
Myc-Vangl2
Flag-p65
IB: α-Myc
F
HA-PDLIM2
Flag-p65
Myc-Vangl2
G
HA-K63+Flag-p65
Pdlim2 siRNA
Myc-Vangl2
CQ+Baf-A1
180kD
H
Vangl2 siRNA
HA-PDLIM2
CQ+Baf-A1
I
LPS
p65 autophagic degradation
K63-Ub
p65
Vangl2
PDLIM2
NDP52
PkBD
NF-κB